Blepharidium guatemalense, an obligate nickel hyperaccumulator plant from non-ultramafic soils in Mexico

Dulce Montserrat Navarrete Gutiérrez, A. Joseph Pollard, Antony van Der Ent, Michel Cathelineau, Marie-Noëlle Pons, Jesús A Cuevas Sánchez, Guillaume Echevarria

Blepharidium guatemalense, an obligate nickel hyperaccumulator plant from non-ultramafic soils in Mexico

Dulce Montserrat Navarrete Gutiérrez[1,2], A. Joseph Pollard [3], Antony van der Ent[1,4], Michel Cathelineau[5], Marie-Noëlle Pons[6], Jesús A. Cuevas Sánchez[2], Guillaume Echevarria[1,4]

[1] Université de Lorraine, INRAE, Laboratoire Sols et Environnement, 54000, Nancy, France.

[2] Universidad Autónoma Chapingo, 56230, Texcoco de Mora, Estado de México, México.

[3] Furman University, Department of Biology, SC 29613, Greenville, USA.

[4] The University of Queensland, Centre for Mined Land Rehabilitation, Sustainable Minerals Institute, QLD 4072, St Lucia, Australia

[5] Université de Lorraine, CNRS, GeoRessources, 54000, Nancy, France.

[6] Université de Lorraine, CNRS, Laboratoire Réactions et Génie des Procédés, 54000, Nancy, France.

*corresponding author: dulce-montserrat.navarrete-gutierrez@univ-lorraine.fr

Telephone: +33(0) 6 11 03 54 46

FAX: +33 (0) 3 83 59 57 91

ACKNOWLEDGEMENTS

The authors acknowledge the Centre National de la Recherche Scientifique (CNRS) in France through the X-LIFE Research Program for their financial support. The first author conveys her sincere gratitude to the Consejo Nacional de Ciencia y Tecnología (CONACyT) in Mexico for PhD funding. GISFI (Université de Lorraine) kindly supplied a hand-held XRF instrument for herbarium scanning. This research was partly undertaken at P06 at at Deutsches Elektronen Synchrotron (DESY), a member of the Helmholtz Association (HGF). The research leading to this result has been also supported by the project CALIPSOplus under the Grant Agreement 730872 from the EU Framework Programme for Research and Innovation HORIZON 2020. The micro-XRF instrumentation used in this study was co-funded by ICEEL (Carnot Institute)-CREGU-LabEX Ressources 21 (ANR-10-LABX 21-LABEX RESSOURCES 21) and FEDER.

Special acknowledgments are made to MSc Blanca V. Juarez Jaimes (MEXU herbarium) for plant identification, to MSc. Jorge A. Ramírez Espinosa, Ing. Francisco Navarrete Torralba and all the students from the Universidad Tecnológica de la Selva (UTS) for their valuable contribution during the field surveys and for their current investment in this research. The authors are also grateful to Haley Disinger for the enrichment of the database (XRF screening data from the MO herbarium in Saint Louis), to Vanessa Invernon for her support at the Paris herbarium (Muséum National d'Histoire Naturelle in Paris) and to all the technicians from MEXU herbarium for their valuable cooperation. We would like to thank Kathryn Spiers and Jan Garrevoet for their assistance during the experiments. We wish to thank Professor Alan Baker (The Universities of Melbourne and Queensland, Australia) for reviewing the paper and suggesting improvements to the text.

DECLARATIONS

The Authors declare that there is no conflict of interest. The content of the manuscript has not been published or submitted for publication elsewhere in any language. All authors have contributed significantly to the realization of the manuscript in different ways.

Abstract

Aims

Nickel hyperaccumulation in *Blepharidium guatemalense* Standl. (Rubiaceae) was found in the tropical forests of south-eastern Mexico. This study aimed to document the geographic extent of nickel hyperaccumulation in this species, to understand its process of hyperaccumulation and to explore nickel distribution within the tissues of this plant.

Methods

Rhizosphere soils and plant tissues were collected in Mexico and analyzed for physical-chemical parameters. Non-destructive elemental screening of herbarium specimens was performed with a hand-held X-ray fluorescence spectrometer. Elemental distribution maps of nickel and other elements in plant tissues were obtained by X-ray fluorescence spectroscopy and microscopy.

Results

Blepharidium guatemalense is distributed throughout Chiapas, Tabasco and Campeche, reaching the maximum nickel concentration in leaves (4.3 wt%) followed by roots and seeds (2.0 wt%) and bark (1.8 wt%). Simultaneous hyperaccumulation of cobalt and nickel was found in 15% of the herbarium specimens. Phloem has the highest nickel-enriched tissue from all parts of the plant (from roots to leaves). A high total nickel (mean of 610 µg g^{-1}) was found in rhizosphere soils even though no evidence of ophiolite emplacement in that area has been reported.

Conclusions

Blepharidium guatemalense has uncommon re-distribution mechanisms *via* phloem. It represents the first hypernickelophore (>1 wt% Ni) to be reported as growing in soils that are neither ultramafic nor enriched by anthropogenic pollutants.

Keywords: *hypernickelophore; XRF scanning; Rubiaceae; biogeochemistry; ionomics; agromining.*

INTRODUCTION

Hyperaccumulator plants actively take up and accumulate metals or metalloids to extremely high concentrations in their above-ground tissues (mostly leaves) when growing in their natural habitats (Baker et al. 1992; van der Ent et al. 2013; Dar et al. 2018). To date, 731 hyperaccumulator species are reported, of which 532 are nickel (Ni) hyperaccumulators (Reeves et al. 2018a; van der Pas and Ingle 2019). The nominal threshold values in plant dry matter depend on the element, *e.g.* 100 µg g^{-1} for cadmium (Cd), 300 µg g^{-1} for cobalt (Co), 1000 µg g^{-1} for Ni, 3000 µg g^{-1} for zinc (Zn) and 10 000 µg g^{-1} for manganese (Mn) (van der Ent et al. 2013). Among these plants, there is a distinct group of about 50 species termed 'hypernickelophores', which can accumulate Ni to concentrations exceeding 1 wt% (10 000 µg g^{-1}) in their shoots (Boyd and Jaffré 2009; Jaffré and Schmid 1974). Hyperaccumulator plants growing on metalliferous soils are classified as 'obligate hyperaccumulators', meanwhile those that are reported to grow (without exhibiting metal hyperaccumulation) in non-metalliferous soils are 'facultative hyperaccumulators' (Pollard et al. 2014). The primary habitats of these hyperaccumulator plants comprise soils developed from the weathering of surficial ore deposits or naturally enriched metalliferous rocks. Most Ni hyperaccumulators grow on soils issued from the weathering of ultramafic rocks, which are the most significant reservoirs of Ni and Co for terrestrial ecosystems (Estrade et al. 2015; Reeves et al. 2018). Since the discovery of the first Ni hyperaccumulator *Odontarrhena* (syn. *Alyssum*) *bertolonii* (Desv.) Jord. & Fourr. (Minguzzi and Vergnano 1948), series of studies of the ultramafic flora provided numerous data on the distribution and number of hyperaccumulator taxa worldwide (Reeves et al. 2018). Most Ni hyperaccumulator plants occur in: i) ultramafic regions around the Mediterranean Basin, especially in Turkey and the Balkans (Brooks et al. 1979; Reeves and Adigüzel 2008), and ii) humid tropical and subtropical ultramafic areas, with three essential hotspots which are Cuba, New Caledonia, and Southeast Asia (Galey et al. 2017; Reeves 2003). According to the Global Hyperaccumulator Database (Reeves et al. 2017), the eight most diverse families in terms of Ni hyperaccumulator species are the Phyllanthaceae (130 spp.), Brassicaceae (104 spp.), Asteraceae (68 spp.), Cunoniaceae (55 spp.), Euphorbiaceae (45 spp.), Salicaceae (39 spp.), Fabaceae (29 spp.) and Rubiaceae (23 spp.).

Mexico is the country with the fourth-largest floristic richness globally, with a record of 23 314 vascular plant species (Villaseñor 2016). These species belong to different families including those also present in the most diverse Ni hyperaccumulator families, such as the Asteraceae (3057 spp.), Fabaceae (1903 spp.), Euphorbiaceae (714 spp.), Rubiaceae (707 spp.), and 10 Brassicaceae (2 spp.)

(Villaseñor 2016). Such diversity suggested the possibility of sear ching for native metal hyperaccumulator plants in Mexico. New techniques for the discovery of hyperaccumulators, such as the non-destructive elemental screening of herbarium specimens through the use of a portable X-ray fluorescence (XRF) instrument, have provided the opportunity to use herbarium specimens to discover new hyperaccumulators (van der Ent et al. 2019a) and new occurrences of mineralized soils.

After several recent attempts to identify Ni hyperaccumulators on ultramafic soils in central and southern Mexico through field surveys, Navarrete Gutiérrez et al. (2018) concluded that Ni hyperaccumulation did not occur in this part of the world. However, a recent XRF screening of herbarium specimens at Missouri Botanical Garden (MO) in Saint Louis, Missouri, USA, revealed for the first time Ni hyperaccumulation in Mexico occurring in several woody species of the genus *Psychotria* (Rubiaceae), namely *Psychotria costivenia* Griseb., *Psychotria lorenciana* C.M. Taylor and *Psychotria papantlensis* (Oerst.) Hemsl., collected in the states of Chiapas, Tabasco and Veracruz (McCartha et al. 2019). These findings led us to undertake new field surveys in these regions and to discover that *Blepharidium guatemalense* Standl. (Rubiaceae) occurs in some of the same communities with the above-mentioned *Psychotria* species, and that also hyperaccumulates Ni (Figure 1). *Blepharidium* is a monospecific genus which was first described in 1918 by Paul Carpenter Standley based upon a type collected in the Department of Alta Verapaz in Guatemala by Henry Pittier in 1905 (Standley 1918). Years later, the species *Blepharidium mexicanum* was reported as a separate species based on taxonomic features such as smaller flowers and sparse pubescence over the lower leaf surface (Standley 1940). Despite morphological differences, *B. mexicanum* is now considered a synonym of *B. guatemalense* (WCSP 2019). The latter is distributed mainly in primary tropical perennial and sub-perennial rainforest of southern Mexico and Guatemala at altitudes ranging from 200 to 500 meters above sea level (m.a.s.l.). 'Popiste' or 'Sayaxché' (as it is called in the local languages), is a hardwood tree up to 70 m in height (Ricked et al. 2013) with a diameter up to 70 cm, and a straight trunk and rounded crown. The outer bark is blue-grey and scaly whereas the inner bark is cream and granular with a total thickness from 5 to 10 cm. Leaves are decussate, oblanceolate 10–30 cm long by 5–12 cm wide. Long and acute stipules occur on younger leaves. The inflorescences are in axillary panicles 10–25 cm long with white flowers and fruits are erect capsules 2–3.5 cm long with abundant brown, flattened and winged seeds 1–1.5 cm long (Pennington and Sarukhán 1968). *Blepharidium guatemalense* is commonly used for rafters, beams and supports of lowland houses due to the strength of its wood whereas its leaves and bark are reputed poisonous (Standley and Williams 1975). The species also grows in secondary forests and on agro-pastoral areas (Ochoa-Gaona et al. 2007; Villanueva López et al. 2015). In the secondary forest, however, *B. guatemalense* appears to be a

pioneer species that colonizes land after many cycles of '*slash* - and - *burn'* which is the ancient cultivation agriculture system still used by local people. In contrast to primary forests, *B. guatemalense* trees are usually between 5–8 m high when growing in secondary forest and in open pasture areas, and they seldom exceed 20 m in these environments. The species is on the IUCN Red List, mainly because of the lack of data (Nelson 1988).

According to existing geological maps, the distribution range of *B. guatemalense* in Guatemala coincides with ultramafic substrates whereas in Mexico its distribution range is derived mainly from limestone, including alluvial and colluvial deposits of the same materials (Ortega-Gutiérrez 1992; SGM 2017). The surprising finding that Ni hyperaccumulation occurs commonly on non-ultramafic soils in south-eastern Mexico was the impetus for this study.

The main purposes of this study were: i) to show the geographic extent of the Ni hyperaccumulation phenomenon in *B. guatemalense*, ii) to understand this phenomenon concerning its rhizosphere soil properties, and iii) to present a first investigation of the Ni distribution within the plant tissues.

MATERIALS AND METHODS

Hyperaccumulation of nickel by *Blepharidium guatemalense* was discovered coincidentally in December 2017 while sampling several species of *Psychotria* in the lowland forests of Chiapas. These *Psychotria* species are priorly reported to hyperaccumulate Ni, hence the interest for Ni hyperaccumulators in this region (McCartha et al. 2019). Therefore, a complete herbarium survey was carried out to determine the extent of Ni hyperaccumulation by this species, followed by a field survey of the interesting regions pointed out by the herbarium study.

Survey of nickel hyperaccumulation by *B. guatemalense* in herbarium specimens

Three herbarium collections were surveyed to get a sufficient distribution of the species in Mexico, these were : MEXU (Mexico City, Mexico), P (Paris, France) and MO (Saint Louis, U.S.A.). Elemental concentrations in mounted herbarium specimens of *B. guatemalense* were measured at the three different herbaria with the same procedure and the same material. The scanning was performed by using a hand-held X-Ray Fluorescence Spectrometer (Thermo Scientific GOLDD+ XL3T-980). The analyzer uses a miniature X-ray tube [Ag anode (6–50 kV, 0–200 µA max] as the primary excitation source and a Silicon Drift Detector (SDD) with 185 eV, 60 000 cps, 4 µs shaping time. It can detect a

range of different elements simultaneously within 30–60 s with a detection limit of 140 µg g^{-1} for most transition elements such as Ni, Cd, Cr, Zn, *etc*. The leaves of dried herbarium specimens were scanned for 30 s in 'soils'" mode and by placing a titanium plate (99.999% purity) underneath the herbarium sheet. During the scanning, specimens are subjected to a beam of high-energy X-rays generated from the X-ray tube; the resulting spectrum of excited fluorescent X-rays serves to detect the elements and to quantify their concentrations.

To obtain better XRF measurement accuracy, calibration and correction of the data were performed. Hence, a total of 256 leaf samples of different Ni (and some concomitantly Zn) hyperaccumulator plant species were collected from different plant species including *B. guatemalense* in the field because it was not possible to achieve destructive sampling of herbarium specimens. Leaf squares of 1 cm^2 in size of each sample were cut and analyzed for 30 s in 'soils' mode with three replicated readings per sample. After XRF measurements, leaf samples were digested and analyzed with Inductively Coupled Plasma Atomic Emission Spectroscopy (ICP-AES) for major and minor elements following the methodology mentioned below in this section.

Paired ICP and XRF data were analyzed by logarithmic linear regression. No noise was detected because the minimum XRF value was about 500 µg g^{-1}, greatly higher than the limit of detection (LOD < 190) estimated by (Gei et al. 2020; van der Ent et al. 2019b). Residuals (observed *vs.* predicted values) were used to detect and remove outliers (± 3 SD of the residual). A secondary linear regression was then derived and transformed to power regression generating the following calibration equation with an R^2 of 0.87:

$$y = 1.1216x^{0.953}$$

where:

Where: x= XRF measurement, y= ICP predicted value

Nickel XRF measurements were finally corrected by using the resulting equation. A calibration equation for Zn ($y = 1.0041x^{0.9316}$ and R^2 of 0.93) was also derived by following the same procedure described above. For Co and Mn XRF measurements, data were corrected by using the calibration equations generated by (Gei et al. 2020): for Co $y = 0.6277x^{1.1706}$ ($r^2 = 0.84$) and for Mn $y = 1.148x^{0.937}$ ($r^2 = 0.73$).

Study and collection sites

<u>*Ocosingo, Chiapas*</u>

In total, 13 sites from the municipality of Ocosingo in Chiapas were sampled. The sites were located in the surroundings of the communities of Lacanhá Chanyasab, San Javier and Cojolita, at altitudes ranging from 100 to 300 m.a.s.l. The area is mainly covered by the "Lacandona" tropical evergreen rainforest, and dominated by rolling hills made up mainly of limestone sedimentary rocks (lutite, limonite) from the upper Cretaceous (Mesozoic) with overlapped layers of marine origin from the lower Tertiary (Cenozoic). Marls and clays could be found on the foot of the slopes and in alluvial areas (Müllerried 1957; Levy Tacher et al. 2006; SGM 2006). Main soil types are Rendzinas, Gleysols and Litosols (INIFAP-CONABIO 1995; Mendoza-Vega and Messing 2005).. Climate is humid warm with abundant rains in summer (Am (i') gw") (García 2004; Köppen 1936)l. The average annual temperature is 25 ° C and total annual precipitation of around 2500 mm (García 2004). The predominant vegetation is evergreen rainforest alternated with secondary vegetation, rain-fed agriculture, and grassland. The first survey took place in December 2017. Promising results from herbarium XRF screenings of *B. guatemalense* leaves from all over south-eastern Mexico prompted a second survey in November 2018 to study some unexplored sites during the first survey in Chiapas.

Tacotalpa, Tabasco

The second survey in November 2018 included the exploration of one site in Tapijulapa, which is a small village belonging to the municipality of Tacotalpa in the southern state of Tabasco. The climate is humid warm with abundant rainfall all year round and an average annual temperature of 26 °C (Af (m) (i) gw") and total rainfall of 3554 mm (Díaz P. et al. 2006; García 2004). Previous predominant vegetation was evergreen rainforest, but this has gradually changed to corn crops, coffee plantations and livestock. Predominant soils are Rendzinas, Humic Acrisols and Eutric Gleysols (CONABIO 2001; INEGI 2005), mainly composed of sedimentary rocks (lutite, limonite, limestone and sandstone). This site was also selected for exploration based on previous data from XRF herbarium screening.

Balancán, Tabasco

Balancán is a municipality located in the eastern part of Tabasco. Climate is humid with summer rains in most of the territory and an average annual temperature of 27 °C (Am (f) (i) gw") (Díaz P. et al. 2006; García 2004; Köppen 1936). Altitude varies from 10 to 50 m.a.s.l. and lands are generally flat with small hills. Vertisol is the main type of soil, derived from sedimentary rocks (sandstone, alluvial deposits) (CONABIO 2001; SGM 2017). Even though many herbarium specimens of *B. guatemalense* presenting high Ni concentrations in their leaves were collected in the municipality of Balancán, no plant could be found in this municipality during the 2018 survey despite many efforts. Main cause could be the drastic woodland reduction from 49 % to 14% that Tabasco suffered over the last 60 years

(Palma-López and Triano 2007). Large surfaces of evergreen rainforest have been converted to grasslands for livestock.

Plant and soil sampling

Soils and plant samples were taken from a total of 14 different sites (13 sites from Chiapas and one from Tabasco) where *B. guatemalense* was found. Most of the studied areas were previously identified from herbarium collections, but some additional areas uncovered by herbarium collections were also surveyed. Three different leaves from a single tree of *B. guatemalense* and its associated rhizosphere soil were taken in the 14 sites for chemical analysis. In some locations, several specimens were collected because we suspected a high variability in Ni concentrations among individual trees. Leaf samples were selected randomly within a plant, and the rhizosphere soil samples were collected near the roots of each individual at a depth of 15 cm. The different types of habitats where samples were collected corresponded to : i) primary evergreen forests, ii) relatively young secondary forests (or fallow fields), and iii) agro-pastoral areas. Other plant tissue samples of *B. guatemalense*, such as fruits (n=9), flowers (n=16), bark (n=25), and roots (n=11) were also collected when available. In addition, one leaf and two seeds of *B. guatemalense* were collected separately, placed into paper bags, and dried in envelopes placed in silica-gel containing bags for Ni distribution analysis within the plant tissues. Some plant specimens were collected in duplicate, numbered, transferred to a press for drying, and prepared as voucher specimens for identification in the MEXU herbarium at Universidad Nacional Autónoma de México (UNAM).

Bulk analysis of plant tissues

Plant tissue samples of *B. guatemalense* were dried at 40 °C for 5 days in a drying oven and subsequently packed for transport to the laboratory for chemical analysis. Dried samples were finely ground (< 250 µm) and subsamples of 0.05 g (± 0.005) were then pre-digested overnight using 1 mL HNO_3 (65%) and 2 mL H_2O_2 (30%). The next day, samples were placed in a heating block (*Digi*PREP) for 2h at 95°C, left to cool to 40 °C, filtered at 0.45µm, and adjusted in volume to 10 mL for minor elements quantification. A 1:10 dilution was carried out with ultrapure water for the quantification of major elements. Finally, digests were analyzed using ICP-AES (Thermo Fisher CAP 6300 Duo). Two blanks and two reference samples of the known hyperaccumulator *Noccaea caerulescens* (J. Presl & C. Presl) F.K. Mey, were used for each analytical series. The same instrument was used in all subsequent ICP-AES analyses.

Bulk analysis of rhizosphere soil samples

Rhizosphere soil samples of *B. guatemalense* collected in the field were air-dried for one week, placed into identified plastic bags and then transported to the laboratory for chemical analysis. Soil pH was measured in a 1:5 soil: water (5 mg soil with 25 mL ultrapure water) suspension after 1 h shaking at 16 rpm and 1h standing. Cation exchange capacity (CEC) of soils was determined using cobalt-hexamine trichloride extraction by adding 50 mL of solution (4.458 g of $Co(NH_3)_6Cl_3$ with 700 mL of distilled water). After 1 h shaking, 10 ml of each sample were filtered at 0.45 µm and measured by spectrophotometry (BioRad, SmartSpec Plus). Available phosphorus (P) was determined according to the Olsen method. For total major and minor elemental quantification, soil samples were dried at 70°C for 3 days in a drying oven and sieved (< 2 mm). Subsequently, 0.5 g (± 0.001 g) of each sample, finely ground (< 250 µm), were digested using 6 mL of 37% HCl and 2 mL of 70% HNO_3 per sample. The acid solution containing soil samples were left to stand overnight before placing on a heating block (*Digi*PREP MS) for 3h at 100°C, and then allowed to cool to a minimum temperature of 40°C. Solutions were adjusted in volume to 45 mL, filtered at 0. 45 µm, and then readjusted to 50 mL with ultrapure water. The final dilution of 1:20 was necessary for major elements. The resulting soil digests/extracts were analyzed by ICP-AES for the quantification of major and minor elements. Trace elements availability in soil samples were determined by using diethylenetriaminepentaacetic acid (DTPA-extractant) according to the method of Lindsay and Norvell, (1978), and then analysis of soil extracts by ICP-AES.

Micro X-ray fluorescence elemental mapping

High spatial resolution (20 µm) distribution maps for Ni and other elements were obtained using a Micro-XRF (M4 Tornado, Bruker). The device has a Rh X-ray tube (50 kV and 200 µA) as a primary excitation source with a Be side window and polycapillary optics. A large and flat sample is subjected to an X-ray beam with a diameter of 20–30 µm inside a chamber under controlled 20 mbar vacuum. X-rays are then detected by two 30 mm^2 Xflash® Silicon Drift detectors (energy resolution of <135 eV at 250 000 cps). A leaf of *B. guatemalense* was collected from its natural habitat in Chiapas and dried at 40 °C for 5 days in a drying oven. Afterwards, a flat section of the leaf (13.0 x 1.9 cm) was cut and analyzed with micro-XRF in the GeoRessources laboratory (France).

X-ray fluorescence microscopy (XFM)

X-ray fluorescence microscopy analysis of different plant tissues of *B. guatemalense* was undertaken at PETRA III (Deutsches Elektronen-Synchrotron; DESY) a 6 GeV synchrotron. The microprobe beamline P06 is equipped with a cryogenically cooled double-crystal monochromator with Si (111) crystals and a K/B mirror focusses a beam of 10^{11} photon/s down to 300 nm size in the energy range

5–21 keV (Schroer et al. 2010).The XRF was collected using a silicon drift detector (Hitachi Vortex EM-90, 80 mm^2, energy-resolution 120 eV) operated in 90-degree geometry). Incident energy of 12 keV was used in order to excite the element of interest with the highest atomic number (*i.e.*, Zn). Different plant tissues (root, stem, petiole, and leaf) of a three-month-old individual of *B. guatemalense*, which was grown in pot experiments under controlled conditions in a Ni-contaminated soil, were analyzed. The samples were hand-cut with a stainless-steel razor blade ('dry knife'), mounted between two sheets of 4 µm 'Ultralene' thin film in a tight sandwich to limit evaporation, and analyzed within 10 minutes after excision. X-ray micro-fluorescence was performed at high speed to keep the scan time to a minimum. The fresh and freeze-dried samples were mounted between two sheets of 'Ultralene' thin film (4 µm) stretched over a perspex frame magnetically attached to the *x*-*y* motion stage at atmospheric temperature (~20 °C). The XRF data were fitted and processed using PyMCA software (Solé et al. 2007), and exported into ImageJ as greyscale 16-bit TIFF files and displayed using ImageJ's 'Fire' lookup table.

Statistical analyses

Soils and plants data were summarized by using Microsoft Excel 2010 (XL STAT ECOLOGY version 2019.1.1) for descriptive statistics, Pearson Correlation Coefficient (*r*) and Principal Components Analysis (PCA). Nickel concentrations are presented as boxplots and in tables. Key symbols: open boxes are inter-quartile ranges, bold crosses are ± mean, whiskers are ± standard deviation and bold circles are outliers. Maps were generated using ArcGIS 10.3.

RESULTS

Elemental concentrations from the herbarium XRF screening in relation to geographical distribution

A total of 182 specimens of *B. guatemalense* historically collected in the current territory of Mexico were scanned by using X-ray fluorescence spectroscopy (XRF); 132 from the MEXU herbarium, 47 from MO and 3 from P. The results revealed the 'obligate' hyperaccumulation character of this species since only 5% of the specimens had Ni concentrations lower than 1000 µg g^{-1}. Yet all the values were > 586 µg g^{-1}, a value higher than the threshold considered to define 'hemi-accumulators' and about 3% of the specimens exceeded the hypernickelophore threshold (10 000 µg g^{-1}). The mean Ni concentration in all 182 specimens was 4022 µg g^{-1} and the maximum Ni concentration of 18 786 µg g^{-1} was recorded in one specimen collected from Ocozocuautla, Chiapas. The histogram shows an approximately log-normal distribution of Ni concentration in the species (Figure 2). Specimens with

available geographical coordinates were georeferenced in a geological map (Figure 3) which confirms that the plant grows across different geological basements but never on ultramafic bedrocks. Ultramafic rock outcrops in Chiapas are found in the southern city of Motozintla, outside the apparent range of distribution of the plant and in a different climatic zone. Occurrences of the species were found on sedimentary formations that include limestone, sandstone, lutite, limonite, marls, clays and alluvial formations derived from the above-mentioned sediments.

Cobalt hyperaccumulation (>300 μg g^{-1}) was found in 27 specimens (*i.e.* 15 %), from which one was collected in Campeche, 11 in Tabasco and 15 in Chiapas with the highest Co concentration of 1994 μg g^{-1} being found in a specimen collected in Tacotalpa, Tabasco. The mean concentration of Co was 446 μg g^{-1} for the 83 specimens that showed values above the detection limit (140 μg g^{-1}). The mean Mn concentration for the 121 specimens with values above the detection limit was 260 μg g^{-1} with a maximum value of 1220 μg g^{-1}. Although they were sometimes high, the concentrations never reached the hyperaccumulation threshold for this metal (*i.e.* 10000 μg g^{-1}). In the case of Zn, the maximum concentration was 476 μg g^{-1}, always well below the hyperaccumulation threshold of 3000 μg g^{-1}. In general, values found for herbarium specimens were lower than in field collected specimens.

Elemental concentrations in plant tissues of *B. guatemalense* collected in the field

The bulk elemental concentrations in the different tissues of *B. guatemalense* are reported for leaves, bark, flowers, fruits, roots and seeds (Table 1). The results were compared with the concentrations of a "reference plant" proposed by Markert (1992). Some major element concentrations were in the expected ranges for most plants in the different plant parts, such as Phosphorus (P), sulphur (S), and magnesium (Mg). Mean potassium (K) concentrations in leaves, flowers and fruits were slightly low (mean < 1.8 wt%), whereas in the roots K concentration barely reached a mean of 0.7 wt%. The highest concentration of K was found in the bark with a maximum concentration exceeding 5.4 wt%. Calcium had typical concentrations in almost all parts of the plant except in the inner bark (with phloem) with a maximum concentration of 3.4 wt%. Copper (Cu) concentrations in the different plant parts were within the normal range (mean < 12 μg g^{-1}). Roots were particularly enriched in aluminium (Al) (mean 3910 μg g^{-1}) and iron (Fe) (mean 4200 μg g^{-1}) compared to other parts of the plant but this could be due to some minor soil contamination, despite thorough rinsing of roots after collection. Leaves showed the highest concentrations from all plant parts, reaching 4.3 wt% Ni (Figure 4) with a mean value of 1.4 wt%, which is beyond the threshold that defines hypernickelophores. The lowest concentration of Ni in the leaves was of 2700 μg g^{-1}. The other parts of the plant also had quite elevated concentrations, especially seeds with a mean Ni concentration of 1.8 wt%. Roots showed a mean Ni

concentration of 1.2 wt% (ranging from 0.2 to 2 wt%) and bark inner tissues (largely phloem) showed the same range as roots (*i.e.* from 0.1 to 1.8 wt% Ni). The lowest Ni concentrations were observed in fruits with a maximum concentration of 4160 µg g^{-1}. Maximum Co accumulation values did not reach the hyperaccumulation threshold (> 300 µg g^{-1}) but exceeded 100 µg g^{-1} in leaves, bark, and roots which were also the parts with maximum Ni accumulation values. Manganese was not accumulated in any of the plant parts and ranged from 22–587 µg g^{-1}, and similarly Zn was not accumulated either with a maximum concentration of 304 µg g^{-1} reported in leaves.

Soil chemistry in the rhizosphere of *B. guatemalense*

Primary habitats of this species correspond mainly to evergreen tropical forests, but it is most often found in secondary forest and in pasture lands where it can be quite abundant. Rhizosphere soil samples from *B. guatemalense* presented different physical properties according to the localities they were collected. Soils from the primary forest were sandy-clay-loam textured, with an olive colour and a granular structure. In the secondary forest, soils were silty-clay textured, exhibiting a grey colour and angular blocks structure. In the pasture lands, they were also silty-clay textured, with an olive colour and a granular structure. The general chemical properties of rhizosphere soil samples were not consistent with an ultramafic origin. Mean pH values for the primary evergreen forest, secondary forest and pasture lands were 6.4, 6.6 and 6.9 respectively. The maximum pH in the primary forest was 6.7, whereas in the secondary forest it was 7.4. Soils revealed a high CEC (mean 40 $cmol^{+}$ kg^{-1}) as expected for tropical clayey soils; the mean total carbon (C) and nitrogen (N) concentrations in soils were 75 g kg^{-1} and 6.16 g kg^{-1}, respectively. Mean exchangeable Ca:Mg ratio was around 4:1. Table 2 shows the total and available concentrations of major and minor elements. High total concentrations were recorded for some metals such as Fe (mean 45 300 µg g^{-1}) and Mn (mean 1380 µg g^{-1}), but concentrations of Co (mean 50 µg g^{-1}) and Zn (mean 65 µg g^{-1}) were within the normal range. Total Ni concentration was surprisingly high for non-ultramafic soils (with a mean value of 610 µg g^{-1}). Mean DTPA-extractable Ni concentration was also very high (and similar to typical concentrations found in ultramafic soils) with a mean value of 50 µg g^{-1}, and the maximum value almost reached 200 µg g^{-1}. Total major nutrient elements were relatively high in the case of Ca (7360 µg g-1) and K (3370 µg g^{-1}). The available P concentrations were moderate (9.4 µg g^{-1}).

Statistical correlations between plant ionomics and rhizosphere soil composition

A Principal Components Analysis (PCA) was performed to reveal the existing relations between the different elemental concentrations in plant leaves and their associated rhizosphere soils collected in the sampling sites. The first three principal components together explained 60.4 % of the total variance,

with 30.5 % of the variance on the first axis, 18.2 % on the second, and 11.7 % on the third. Projections of factor scores and loadings for the first and second components are presented in Figure 5. There was no apparent relation among soil and plant variables, except for a positive association between Ni concentration in leaves and the available Ni content in soils (r = 0.510). Three Pearson correlation coefficients were obtained separately: i) plant elemental concentrations, ii) total elemental contents in soils and iii) DTPA-extractable concentrations in soils. Within plant leaves, Ni was highly positively related with Zn (r = 0.970). Other strong positive correlations could be observed, such as Ca-Mg (r = 0.807). In soils, CEC was positively correlated with the N (r = 0.766) and C (r = 0.775) contents in soils. Pearson correlation matrix with all the significant correlations is shown in Appendix 1.

Desktop fluorescence microscopy on plant tissues

The micro-XRF maps show the spatial distribution of Ni and other elements in one leaf and two seeds of *B. guatemalense*. Elemental maps revealed a much higher signal of Ni in the midrib and veins of leaves with a lower signal in the epidermis (Figure 6). Calcium was present all over the leaf whereas K, Fe, Zn and Mn were mainly present in the midrib and secondary veins, similarly to Ni. As opposed to Ni, Co, Mg and S were detectably higher in the leaf blade than in the veins. The elemental map of seeds revealed that Ca and K were homogeneously distributed throughout the wing that envelops the seed with a higher signal in the pericarp. A high Ni signal was detected in the pericarp with a maximum intensity in the seed embryo.

Elemental localization in plant tissues by XFM

Maps generated by XFM technology enabled us to elucidate the elemental localization in the organs of the different plant tissues (root, stem, petiole and leaf midrib) of *B. guatemalense*. The results showed that Ni was highly concentrated in the phloem of all plant tissues. In the leaf midrib cross-section (Figure 7 a), Ni was mainly enriched in the collenchyma, followed by in the primary and secondary veins (phloem) and the parenchyma of the leaf blade. Zinc followed the same distribution pattern as Ni but with a lower intensity. Calcium spots were probably calcium oxalate crystals in all plant tissues as observed in many plants (van der Ent et al. 2017). The mesophyll was strongly enriched in Ca all along the leaf blade. Potassium was uniformly distributed throughout the leaf. In the petiole cross-section (Figure 7 b), Ni was enriched in the phloem but highest in the sclerenchyma cells of the cortex. Zinc occurs similarly to Ni but was also found in the xylem. Calcium and K were mainly distributed in the phloem and the cortex. In the stem cross-section (Figure 7 c) Ni was strongly enriched in the phloem and in the cambium, but only moderately enriched in the cell walls of the cortex, in the primary xylem and in the parenchymal cell walls of the pith. Zinc distribution matches (again) that of

Ni but with a noticeably higher enrichment in the primary xylem. Potassium was poorly concentrated in the primary xylem and secondary phloem. There was a strong enrichment of Ca in the phloem and in the parenchyma cells of the pith. In the root cross-section (Figure 7 d), the Ni was particularly highly enriched in the phloem, in the endoderm and in the epidermis. Nickel was also present in the xylem but at lower concentrations. Potassium was moderately enriched in the epidermis. Zinc is localized at a low concentration in the phloem being highest in the epidermis. Calcium is depleted in the cortex but strongly enriched in the phloem and in the epidermis.

DISCUSSION

Ecology and occurrence of *B. guatemalense* in Mexico

Many sites in Tabasco (*e.g.* Balancan region), where *B. guatemalense* was often collected three decades before, suffered a dramatic land-use changes. The evergreen rainforest cleared to develop cattle grassland, reducing its geographic distribution to the areas where traditional agriculture co-exists with secondary and sometimes primary forests. For this reason, the survey of the species in the lowlands of Campeche was abandoned. It turned out that it was impossible to find the species at any of the collection locations of herbarium specimens in the Balancan Region and other lowland regions of Tabasco. However, *B. guatemalense* still occurs over a broad range of ecosystems across the state of Chiapas, from Palenque down to the Usumacinta valley and the Lacandona Forest. In Tabasco, it can only be found in the extreme southern part of Tabasco close to the border with Chiapas where the landscape becomes hilly and soils are developed on limestone (Tapijulapa region). Its current distribution advocates for removing this species from the IUCN Red List as it is still very widely distributed and very common in the occurring areas which cover thousands of sq. km. Moreover, it is commonly used by local communities for roofing and selectively maintained in pastures to harvest the tree for poles.

Although all the soils where this species was sampled were highly enriched in Ni, Fe and Mn, as it is probably the case in this entire lowland region of Mexico (Hernández-Quiroz *et al*. 2012), they did not form from ultramafic bedrock (Ortega-Gutiérrez 1992; SGM 2006). The soils have no apparent deficiency in Ca or in the other essential macronutrients (N, K, P), by contrast with ultramafic soils (Proctor 2003). Mean total Ni concentration in the first cm of the soils is well above the limit of Ni concentration recommended in soils from the USA (i.e. 210 µg g^{-1}) and the toxicity threshold specified by the Mexican norm NOM-147-SEMARNAT/SSA1-2004 (i.e. 1600 µg g^{-1}). A potential source of Ni in these soils could be lateritic material transported by water from the ultramafic complexes occurring

throughout the Polochic-Motagua fault systems in Guatemala. Hernández-Quiroz *et al*. (2012) proposed that the main sources of Ni (39–318 µg g^{-1}) in similar soils collected near a petrochemical facility in Tabasco were either volcanic material deposits or lateritic nodular fragments (associated with crystalline Fe oxides and the residual fraction). The latter materials were transported from preexisting soils (pedorelicts), possibly formed out from ultramafic rocks situated in the margins of the Caribbean plate in ancient times. Another significant contributor to the current Ni concentration in soils could be the volcanic ash deposits derived from the constant activity of the nearest volcanos, e.g. El Chichón and Tacaná. Nevertheless, further mineralogical studies are needed to answer these questions and to better characterize these unusual soils. In any case, the presence of elevated soil Ni in localities scattered throughout this region probably explains the extension of *B. guatemalense* and other associated Ni-hyperaccumulators (*e.g. Psychotria costivenia*, *P. lorenciana* and *P. papantlensis*) (McCartha et al. 2019).

Nickel hyperaccumulation in *B. guatemalense* and its significance

Non-destructive hand-held XRF technology is an excellent example of these promising new tools which has permitted the addition of many hyperaccumulator taxa to the global inventory in the recent years (Gei et al. 2018). Extensive systematic screenings of mounted specimens in different herbaria have been performed including at the FRC Herbarium in Sabah (Malaysia) and the IDR Herbarium in Nouméa (New Caledonia) with the discovery of 85 and 91 new hyperaccumulator taxa respectively (van der Ent et al. 2019a, b; Gei 2020).

Data obtained from the XRF herbarium scanning confirmed the obligate hyperaccumulation trait in this species because only 5.5% of the herbarium specimens had Ni concentrations below the hyperaccumulation threshold. Mean Ni concentrations in the leaves of *B. guatemalense* scanned in the herbaria were considerably lower than those collected in the field. In field-collected plants, *Blepharidium guatemalense* was, therefore, able to accumulate among the highest Ni concentrations reported in hyperaccumulator leaves globally, which places it in the group of 'hypernickelophores' plants (*i.e.* >1% wt) (Boyd and Jaffré 2009; Reeves et al. 2018b).

Until now, Ni hyperaccumulator species belonging to the Rubiaceae family had been only reported in the well-known tropical hotspots of biodiversity such as the neighbouring territory of Cuba (11 spp), New Caledonia (3 spp) and Malaysia (3 spp). Within the Rubiaceae, the tribe *Rondeletieae* (Manns and Bremer 2010; Rova et al. 2009) includes *Blepharidium* along with at least three other genera of hyperaccumulators reported from Cuba by Reeves et al. (1999): *Rondeletia*, *Phyllomelia* and *Mazanea*

(= *Ariadne*) or newly discovered hyperaccumulators in the genus *Arachnothryx* (formerly *Rondeletia*) in central America (Nkrumah et al., 2021). Further herbarium surveys on phylogenetically close genera/species of known hyperaccumulators in Mexico could lead to the discovery of new hyperaccumulator taxa.

Level of uptake of Ni and Co by *B. guatemalense* from surrounding soils

The heterogeneous distribution of DTPA-extractable Ni in soils could explain the high variability in Ni concentrations within foliar samples collected in the field as those two variables were positively correlated. No other soil characteristics seemed to influence Ni uptake. An old pasture which had the maximum DTPA-extractable Ni concentration showed a high density of *B. guatemalense* clustered in patches of around 10 m in diameter. Because of the high heterogeneity of Ni availability in soils resulting from the similar geological and pedological situation, one can question whether the presence of the species itself influences the variability of Ni levels through biogeochemical recycling. The highly concentrated large leaves from fast-growing trees suggest, among other factors, that litter produced by *B. guatemalense* could contribute significantly to the available Ni pool in the surface soils, These changes in Ni concentrations could, in turn, offer a suitable habitat for other Ni hyperaccumulator plants. Indeed, in primary and secondary forests in our study area, *B. guatemalense* was frequently observed accompanied by the facultative Ni-hyperaccumulator *Psychotria costivenia* as an understory plant beneath it. Preliminary observations suggested that shrubs of *P. costivenia* growing under *B. guatemalense* trees have much higher Ni concentrations than those that are not under such a canopy.

Simultaneous Ni and Co hyperaccumulation was reported in 27 mounted specimens from the MEXU and MO herbaria with a ratio of ~ 8:1 Ni:Co. Similar cases of simultaneous Ni and Co hyperaccumulation have been observed in the Malaysian tree *Glochidion* cf. *sericeum* (Phyllanthaceae) with an unusual ratio of 1:1 Ni:Co. Another example is *Rinorea bengalensis* (Wall.) Kuntze (Violaceae) with Co values up to 630 µg g^{-1}, also found by XRF scanning or *Berkheya coddii* (Asteraceae), with Co values higher than 600 µg g^{-1} (Lange et al. 2017). Nevertheless, the Co concentration in foliar samples of *B. guatemalense* collected in the field did not reach hyperaccumulation threshold. This may be due to the almost neutral pH in rhizosphere soils, since it is known that plants accumulate Co mostly in acidic substrata (Kukier et al. 2004), but also to the competition between Ni and Co for uptake mechanisms, as described for *Alyssum* species and *B. coddii* (Homer et al. 1991; Keeling et al. 2003).

Elemental distribution in *B. guatemalense* and physiological aspects

On sufficiently old trunks, the inner bark of the tree that is in direct contact with wood (phloem tissues) on trunks that are old enough shows a particular turquoise green-blue colour due to high Ni concentrations. Such an intense green colour is one of the most outstanding features of woody Ni hyperaccumulators that has been also observed in some South Eastern Asian and Pacific species (*e.g. Phyllanthus balgooyi* Petra Hoffm. & A.J.M.Baker, and *R. bengalensis*), and is due to the very high concentrations of Ni^{2+} ions in this tissue (van der Ent et al. 2017a). Nickel-enriched phloem tissues on the stem of the South African Ni hyperaccumulator *Senecio coronatus* (Thunb.) Harv. have also been reported (Mesjasz-Przybylowicz 1997). Desktop micro-XRF showed rather heterogeneous distributions of Ni across the leaf in both veins and leaf blades. The XFM elemental maps confirmed the high Ni concentrations, not only in the phloem of the primary (leaf midrib) and secondary leaf veins, but also in the phloem of the root, stem and petiole. As for other species which show this specific feature, *e.g. P. balgooyi* (van der Ent et al. 2017b) or *R. bengalensis* (Zelano et al. *in press*), *B. guatemalense* appears to redistribute Ni within the plant *via* the phloem. Phloem active transport of Ni was confirmed in another Ni hyperaccumulator *Noccaea caerulescens* by using Ni stable isotope analysis (Deng et al. 2016, 2018).

Another fact that confirms the re-distribution of Ni *via* phloem in *B. guatemalense* is the high Ni concentrations reported in flowers and fruits, and extremely high values in seeds. Indeed, the only pathway for Ni (and eventually other heavy metals) to reach sink organs (maturing fruits, seeds, flowers, *etc.*) is through the mass movement of phloem fluids coming from the source organs (senescing leaves) (Bhatia et al. 2003; Page and Feller 2015). Leaf epidermal cells of *B. guatemalense* were not Ni enriched as opposed to most hyperaccumulator species; this trait was also observed for the following species: *Berkheya coddii* and *P. balgooyi* (van der Ent et al. 2017).

According to the updated knowledge on Ni hyperaccumulators which redistribute Ni through the phloem, we could hypothesize that Ni^{2+} could be loaded into the xylem as the free cation and transported to the shoots where it may be complexed by carboxylic acids (mainly citrate), and partly stored in the leaf midrib collenchyma (van der Pas and Ingle 2019). Since a slight Ni accumulation is observed in the leaf parenchyma, transport may also occur from the xylem to mesophyll cells in the transpiration stream (Page and Feller 2015). In minor leaf veins, Ni may also be transferred directly from the xylem to the phloem through companion cells (Page and Feller 2015; van Bel 1990). In many Ni hyperaccumulators globally, Ni^{2+} is complexed predominantly by citrate or malate in leaves, phloem or latex and its chemical speciation does not substantially change among different plant tissues

589 (van der Ent et al. 2017). Sugars, amino acids and organic acids are expected to be the most
590 predominant metabolites in the phloem sap (Braun et al. 2014). The dominant Ni-citrate complexes in
591 the phloem tissues of *P. balgooyi* seem to be associated with low sugar contents (mainly sucrose) (van
592 der Ent et al. 2017). In this case, higher sucrose concentration in the mesophyll cell cytoplasm may
593 enhance the passive loading of the phloem moving by diffusion down its concentration gradient to the
594 sieve-tube elements. Such a process could explain the higher Ni concentration in the phloem tissues
595 than in the leaves in this species, as it could be the case in *B. guatemalense*. Conversely, *P.*
596 *rufuschaneyi* accumulated higher Ni accumulation in leaves with respect to phloem tissues (van der
597 Ent et al. 2017). This highlights that further studies on the Ni chemical speciation in the different
598 tissues and fluids of *B. guatemalense,* including phloem sap, are crucial to better understand these
599 processes at the cellular level.
600
601 In the leaf samples taken in the field, cobalt was accumulated at close-to-hyperaccumulation levels in
602 the leaf samples taken in the field for micro-XRF analysis. In Co hyperaccumulators, Co is sometimes
603 found in the form of lesions in the leaf surface as a result of an extracellular detoxification mechanism
604 *via* exudation of guttation liquids (van der Ent et al. 2018), whereas it is found accumulated at the leaf
605 tip in *Alyssum murale* (syn. *Odontarrhena chalcidica*) (Tappero et al. 2007). No evidence of these
606 lesions or of tip accumulation was observed in the micro-XRF distribution map of *B. guatemalense*
607 because of the low Co concentration in the foliar samples collected in the field. Pearson correlation
608 coefficient (*r*) of foliar elemental concentrations showed a strong positive correlation between Ni and
609 Zn (Spearman test, p value < 0.0001). Both elements can, therefore, enter through the plasma
610 membrane of root cells *via* the same poorly selective cation transporter members of the ZIP gene
611 family (van der Pas and Ingle 2019). Also, the distribution of Zn matches with that of Ni within the
612 different plant tissues, as observed in the XFM elemental maps.
613
614 **Potential applications for *B. guatemalense***
615 *Blepharidium guatemalense* possess the required characteristics to be an excellent candidate for Ni
616 agromining (phytomining), such as being a hypernickelophore, high biomass, apparent fast-growth
617 rate and easy reproduction (Nkrumah et al. 2018). The fact that the wood of this species is currently
618 used for building (*e.g.* rafters, beams and supports of houses) by local populations in Chiapas and
619 Tabasco supports the idea that the wood of hyperaccumulator plants may be durable against termites
620 by acting as natural insecticide/fungicide (van der Ent and Mulligan 2015). Our observations also
621 suggest the possibility of further agromining implementation in secondary forest and pasturelands
622 where the tree is grown (or left to grow) in a deliberate way. Sustainable agromining systems using *B.*

guatemalense could contribute to the preservation of this unique species. Research is currently underway to study the agronomy of this species and the environmental, social and economic implications of any implementation of agromining in those regions.

CONCLUSIONS

Blepharidium guatemalense, a new obligate hypernickelophore species able to accumulate up to 4.3 wt.% Ni in its leaves, was discovered in south-eastern Mexico thanks to herbarium screening and field sampling. It was found in the States of Tabasco, Chiapas and Campeche. Inner bark samples of older trees show a typical green colour and Ni was shown to be uniformly distributed in the leaf but with higher concentrations in the midrib and in the secondary veins. Phloem tissues were identified with XFM techniques as the major sink of Ni in this tree, suggesting active internal re-distribution mechanisms similar to those reported in other extreme tropical Ni-hyperaccumulator species with green phloem sap.

Prior this research, no 'hypernickelophore' had ever been reported on non-ultramafic soils. *Blepharidium guatemalense* does so consistently, over a vast region of south-eastern Mexico that is covered by sedimentary geological layers, although showing elevated geochemical backgrounds in Ni and associated elements. Moreover, in the natural lowland forests of Chiapas, stands of *B. guatemalense* may create Ni-rich habitats for other Ni hyperaccumulator species growing underneath (*e.g. P. costivenia*) likely by recycling Ni through the decay of Ni-rich litter in the topsoil. This finding shifts the paradigm and enables the exploration of 'natural' Ni hyperaccumulator habitats beyond the constraints of ultramafic geology. Pioneering investigations are being carried out to study the application of *B. guatemalense* for Ni agromining (phytomining).

ACKNOWLEDGEMENTS

The authors are grateful to the following herbaria for access to the collections and support: Museum National d'Histoire Naturelle (P), Missouri Botanical Gardens (MBG) and Universidad Nacional Autónoma de México (MEXU). They are also grateful to the Groupement d'Intérêt Scientifique sur les Friches Industrielles (GISFI) from the Université de Lorraine for providing key support with the use of the portable X-ray Fluorescence apparatus and to the X-LIFE programme of the French National Centre for Scientific Research (CNRS) which funded herbarium screening for hyperaccumulators and field trips to Mexico (X-TREM project). In particular, they wish to thank Dr. Sylvain Merlot (IB2C, CNRS), scientific coordinator of the X-TREM project. The XFM analysis of fresh plant sections was undertaken at P06 at DESY, a member of the Helmholtz Association (HGF). The National Council of

657 Science and Technology (CONACYT) in Mexico and the French National Research Agency, reference
658 ANR-10-LABX-21 - LABEX RESSOURCES21 are also acknowledged for funding the PhD
659 scholarship of Dr Dulce Navarrete Gutiérrez.

660

661 **REFERENCES**

662

663 Baker AJM, Proctor J, Reeves RD (1992) Hyperaccumulation of Nickel by the Flora of the
664 Ultramafics of Palawan, Republic of the Philippines. In: The Vegetation of Ultramafic
665 (Serpentine) Soils. p 14

666 Bhatia NP, Orlic I, Siegele R, et al (2003) Elemental mapping using PIXE shows the main pathway
667 of nickel movement is principally symplastic within the fruit of the hyperaccumulator
668 *Stackhousia tryonii*. New Phytol 160:479–488. https://doi.org/10.1046/j.1469-
669 8137.2003.00912.x

670 Boyd RS, Jaffré T (2009) Elemental concentrations of eleven New Caledonian plant species from
671 serpentine soils : elemental correlations and leaf-age effects. Northeast Nat 16:93–110.
672 https://doi.org/10.1656/045.016.0508

673 Braun DM, Wang L, Ruan Y-L (2014) Understanding and manipulating sucrose phloem loading,
674 unloading, metabolism, and signaling to enhance crop yield and food security. J Exp Bot
675 65:1713–1735. https://doi.org/10.1093/jxb/ert416

676 Brooks RR, Morrison RS, Reeves RD, et al (1979) Hyperaccumulation of nickel by *Alyssum*
677 *Linnaeus* (Cruciferae). Proc R Soc Lond B Biol Sci 203:387–403.
678 https://doi.org/10.1098/rspb.1979.0005

679 Dar MI, Naikoo MI, Green ID, et al (2018) Heavy Metal Hyperaccumulation and Hypertolerance in
680 Brassicaceae. In: Hasanuzzaman M, Nahar K, Fujita M (eds) Plants Under Metal and
681 Metalloid Stress: Responses, Tolerance and Remediation. Springer, Singapore, pp 263–276

682 Deng T-H-B, Tang Y-T, van der Ent A, et al (2016) Nickel translocation via the phloem in the
683 hyperaccumulator *Noccaea caerulescens* (Brassicaceae). Plant Soil 404:35–45.
684 https://doi.org/10.1007/s11104-016-2825-1

685 Deng T-H-B, van der Ent A, Tang Y-T, et al (2018) Nickel hyperaccumulation mechanisms: a
686 review on the current state of knowledge. Plant Soil 423:1–11.
687 https://doi.org/10.1007/s11104-017-3539-8

688 Díaz P. G, Ruiz C. JA, Medina G., G, et al (2006) Estadísticas Climatológicas Basicas del estado de
689 Tabasco (Periodo 1961-2003). Veracruz, México.

690 Estrade N, Cloquet C, Echevarria G, et al (2015) Weathering and vegetation controls on nickel
691 isotope fractionation in surface ultramafic environments (Albania). Earth Planet Sci Lett
692 423:24–35. https://doi.org/10.1016/j.epsl.2015.04.018

693 Galey ML, van der Ent A, Iqbal MCM, Rajakaruna N (2017) Ultramafic geoecology of South and
694 Southeast Asia. Bot Stud 58:. https://doi.org/10.1186/s40529-017-0167-9

695 García E (2004) Modificaciones al Sistema de Clasificación Climática de Köppen, 5th edn. Instituto
696 de Geografía, Universidad Nacional Autónoma de México.

Gei V, Erskine PD, Harris HH, et al (2018) Tools for the discovery of hyperaccumulator plant species and understanding their ecophysiology. In: Van der Ent A, Echevarria G, Baker AJM, Morel JL (eds) Agromining: Farming for Metals: Extracting Unconventional Resources Using Plants. Springer International Publishing, Cham, pp 117–133

Gei V, Isnard S, Erskine PD, et al (2020) A systematic assessment of the occurrence of trace element hyperaccumulation in the flora of New Caledonia. Bot J Linn Soc *In press*:

Hernández-Quiroz M, Herre A, Cram S, et al (2012) Pedogenic, lithogenic or anthropogenic origin of Cr, Ni and V in soils near a petrochemical facility in Southeast Mexico. Catena 93:49–57. https://doi.org/10.1016/j.catena.2012.01.005

Homer FA, Morrison RS, Brooks RR, et al (1991) Comparative studies of nickel, cobalt, and copper uptake by some nickel hyperaccumulators of the genus *Alyssum*. Plant Soil 138:195–205. https://doi.org/10.1007/BF00012246

INEGI (2005) Marco Geoestadístico Municipal 2005. Prontuario de Información Geográfica Municipal (Tacotalpa, Tabasco).

INIFAP-CONABIO (1995) (1995) Edafología, escalas 1:250000 - 1:1000000

Jaffré T, Schmid M (1974) Accumulation du nickel par une Rubiacée de Nouvelle-Callédonie, *Psychotria douarrei* (G. Beauvisage) Däniker. 1727–1730

Keeling SM, Stewart RB, Anderson CWN, Robinson BH (2003) Nickel and Cobalt Phytoextraction by the Hyperaccumulator *Berkheya coddii* : Implications for Polymetallic Phytomining and Phytoremediation. Int J Phytoremediation 5:235–244. https://doi.org/10.1080/713779223

Köppen W (1936) Das geographische System der Klimate. Borntraeger, Berlin: Gebrüder Borntraeger.

Lange B, Ent A van der, Baker AJM, et al (2017) Copper and cobalt accumulation in plants: a critical assessment of the current state of knowledge. New Phytol 213:537–551. https://doi.org/10.1111/nph.14175

Levy Tacher SI, Aguirre Rivera JR, García Perez JD, Martínez Romero MM (2006) Aspectos florísticos de Lacanhá Chansayab, Selva Lacandona, Chiapas. Acta Botánica Mex 69–98

Lindsay WL, Norvell WA (1978) Development of a DTPA soil test for zinc, iron, manganese, and copper. Soil Sci Soc Am J 42:421. https://doi.org/10.2136/sssaj1978.03615995004200030009x

Markert B (1992) Establishing of "Reference Plant" for inorganic characterization of different plant species by chemical fingerprinting. Water Air Soil Pollut 64:533–538. https://doi.org/10.1007/BF00483363

McCartha GL, Taylor CM, Ent A, et al (2019) Phylogenetic and geographic distribution of nickel hyperaccumulation in neotropical *Psychotria*. Am J Bot 106:1377–1385. https://doi.org/10.1002/ajb2.1362

733 Mendoza-Vega J, Messing I (2005) The influence of land use and fallow period on the properties of
734 two calcareous soils in the humid tropics of southern Mexico. Catena 60:279–292.
735 https://doi.org/10.1016/j.catena.2004.12.002

736 Mesjasz-Przybyłowicz J, Przybyłowicz WJ, Prozesky VM, Pineda CA (1997) Quantitative micro-
737 PIXE comparison of elemental distribution in Ni-hyperaccumulating and non-accumulating
738 genotypes of *Senecio coronatus*. Nucl Instrum Methods Phys Res Sect B Beam Interact
739 Mater At 130:368–373. https://doi.org/10.1016/S0168-583X(97)00228-0

740 Müllerried FKG (1957) La Geología de Chiapas. Gobierno Constitucional del Estado de Chiapas

741 Navarrete Gutiérrez DM, Pons M-N, Cuevas Sánchez JA, Echevarria G (2018) Is metal
742 hyperaccumulation occurring in ultramafic vegetation of central and southern Mexico? Ecol
743 Res 33:641–649. https://doi.org/10.1007/s11284-018-1574-4

744 Nelson C (1988) *Blepharidium guatemalense. The IUCN Red List of Threatened Species 1998*:
745 e.T30687A9566678. http://dx.doi.org/10.2305/IUCN.UK.1998.RLTS.T30687A9566678.en.

746 Nkrumah PN, Chaney RL, Morel JL (2018) Nkrumah et al. - 2018a - Agronomy of 'Metal Crops'
747 Used in Agromining.pdf. In: Van der Ent A, Echevarria G, Baker AJM, Morel JL (eds)
748 Agromining: Farming for Metals: Extracting Unconventional Resources Using Plants.
749 Springer International Publishing, Cham, pp 19–38

750 Nkrumah PN, Navarrete Gutiérrez DM, Tisserand R, van der Ent A, Echevarria G, Pollard AJ,
751 Chaney RL, Morel JL (2021) Element Case Studies: Nickel (Tropical Regions). In: Van der
752 Ent A, Baker AJM, Echevarria G, Simonnot MO, Morel JL (eds) Agromining: Farming for
753 Metals: Extracting Unconventional Resources Using Plants (2nd Edition). Mineral Resources
754 Reviews, Springer International Publishing, Cham, pp 365–383

755 Ochoa-Gaona S, Hernández-Vázquez F, Jong BHJD, Gurri-García FD (2007) Pérdida de diversidad
756 florística ante un gradiente de intensificación del sistemaagrícola de roza-tumba-quema: un
757 estudio de caso en la Selva Lacandona, Chiapas, México. Bot Sci 65–80.
758 https://doi.org/10.17129/botsci.1766

759 Ortega-Gutiérrez F (1992) Carta geológica de la República Mexicana. [Mexico, D.F.]: Consejo de
760 Recursos Minerales y en el Instituto de Geología de la UNAM.

761 Ortiz-Hernández LE, Escamilla-Casas JC, Flores-Castro K, et al (2006) Características geológicas y
762 potencial metalogenético de los principales complejos ultramáficos-máficos de México. Bol
763 Soc Geológica Mex LVIII:161–181

764 Page V, Feller U (2015) Heavy metals in crop plants: transport and redistribution processes on the
765 whole plant level. Agronomy 5:447–463. https://doi.org/10.3390/agronomy5030447

766 Palma-López, D., Triano S., A., 2007. Plan de uso sustentable de los suelos de Tabasco. Vol. II, 2nda
767 Reimpresión. ed. COLEGIO DE POSTGRADUADOS-ISPROTAB, Villahermosa, Tabasco.
768 México. 180 p.

769 Pennington TD, Sarukhán J (2005) Árboles tropicales de México: manual para la identificación de
770 las principales especies., 3rd edn. Universidad Autónoma de México, & Fondo de Cultura
771 Económica (Mexico), México, Distrito Federal

772 Pollard AJ, Reeves RD, Baker AJM (2014) Facultative hyperaccumulation of heavy metals and
773 metalloids. Plant Sci 217–218:8–17. https://doi.org/10.1016/j.plantsci.2013.11.011

774 Proctor J (2003) Vegetation and soil and plant chemistry on ultramafic rocks in the tropical Far East.
775 Perspect Plant Ecol Evol Syst 6:105–124. https://doi.org/10.1078/1433-8319-00045

776 Reeves R, Baker AJM, Jaffré T, et al (2018a) A global database for plants that hyperaccumulate
777 metal and metalloid trace elements. New Phytol 218:407–411.
778 https://doi.org/10.1111/nph.14907

779 Reeves RD (2003) Tropical hyperaccumulators of metals and their potential for phytoextraction.
780 Plant Soil 249:57–65. https://doi.org/10.1023/A:1022572517197

781 Reeves RD, Adigüzel N (2008) The Nickel Hyperaccumulating Plants of the Serpentines of Turkey
782 and Adjacent Areas: A Review with New Data. Turk J Biol Year 2008 Vol 32 Issue 3 143-
783 153

784 Reeves RD, Baker AJM, Borhidi A, Berazaín R (1999) Nickel hyperaccumulation in the serpentine
785 flora of Cuba. Ann Bot 83:29–38. https://doi.org/10.1006/anbo.1998.0786

786 Reeves RD, van der Ent A, Baker AJM (2018c) Global Distribution and Ecology of
787 Hyperaccumulator Plants. In: Van der Ent A, Echevarria G, Baker AJM, Morel JL (eds)
788 Agromining: Farming for Metals: Extracting Unconventional Resources Using Plants.
789 Springer International Publishing, Cham, pp 75–92

790 Ricked M, Hernández HM, Sousa M, Ochoterena H (2013) Tree and tree-like species of Mexico:
791 Asteraceae, Leguminosae, and Rubiaceae. Rev Mex Biodivers 84:439–470.
792 https://doi.org/10.7550/rmb.32013

793 Rova JHE, Delprete PG, Bremer B (2009) The *Rondeletia* complex (Rubiaceae): an attempt to use
794 ITS, rps16, and trnL-F sequence data to delimit Guettardeae, Rondeletieae, and sections
795 within Rondeletia 1. Ann Mo Bot Gard 96:182–193. https://doi.org/10.3417/2006179

796 Schroer CG, Boye P, Feldkamp JM, et al (2010) Hard X-ray nanoprobe at beamline P06 at PETRA
797 III. Nucl Instrum Methods Phys Res Sect Accel Spectrometers Detect Assoc Equip 616:93–
798 97. https://doi.org/10.1016/j.nima.2009.10.094

799 SGM (2017) Cartografía Geológica de la República Mexicana escala 1:250,000.

800 SGM (2006) Carta Geológica Minera “Las Margaritas” E15-12 D15-3 Chiapas

801 Solé VA, Papillon E, Cotte M, et al (2007) A multiplatform code for the analysis of energy-
802 dispersive X-ray fluorescence spectra. Spectrochim Acta Part B At Spectrosc 62:63–68.
803 https://doi.org/10.1016/j.sab.2006.12.002

804 Standley PC (1940) Rubiaceae, *Blepharidium*. In: Studies of American plants-X. Field Museum of
805 Natural History, Chicago [Ill.], pp 108–109

806 Standley PC (1918) *Blepharidium*, a new genus of Rubiaceae from Guatemala. J Wash Acad Sci
807 8:58–60

Standley PC, Williams LO (1975) *Blepharidium* Standley. In: Flora of Guatemala. Field Museum of Natural History, Chicago, [Ill.], pp 17–18

Tappero R, Peltier E, Gräfe M, et al (2007) Hyperaccumulator *Alyssum murale* relies on a different metal storage mechanism for cobalt than for nickel. New Phytol 175:641–654. https://doi.org/10.1111/j.1469-8137.2007.02134.x

van Bel AJE (1990) Xylem-phloem exchange via the rays: the undervalued route of transport. J Exp Bot 41:631–644. https://doi.org/10.1093/jxb/41.6.631

van der Ent A, Baker AJM, Reeves RD, et al (2013) Hyperaccumulators of metal and metalloid trace elements: facts and fiction. Plant Soil 362:319–334. https://doi.org/10.1007/s11104-012-1287-3

van der Ent A, Callahan DL, Noller BN, et al (2017b) Nickel biopathways in tropical nickel hyperaccumulating trees from Sabah (Malaysia). Sci Rep 7:41861. https://doi.org/10.1038/srep41861

van der Ent, A. van der, Echevarria, G., Pollard, A.J., Erskine, P.D., 2019a. X-Ray Fluorescence Ionomics of Herbarium Collections. Sci. Rep. 9, 1–5. https://doi.org/10.1038/s41598-019-40050-6

van der Ent A, Mak R, Jonge MD de, Harris HH (2018) Simultaneous hyperaccumulation of nickel and cobalt in the tree *Glochidion cf. sericeum* (Phyllanthaceae): elemental distribution and chemical speciation. Sci Rep 8:1–15. https://doi.org/10.1038/s41598-018-26891-7

van der Ent A, Mulligan D (2015) Multi-element concentrations in plant parts and fluids of Malaysian nickel hyperaccumulator plants and some economic and ecological considerations. J Chem Ecol 41:396–408. https://doi.org/10.1007/s10886-015-0573-y

van der Ent, A., Ocenar, A., Tisserand, R., Sugau, J.B., Echevarria, G., Erskine, P.D., 2019b. Herbarium X-ray fluorescence screening for nickel, cobalt and manganese hyperaccumulator plants in the flora of Sabah (Malaysia, Borneo Island). J. Geochem. Explor. 202, 49–58. https://doi.org/10.1016/j.gexplo.2019.03.013

van der Pas L, Ingle RA (2019) Towards an understanding of the molecular basis of nickel hyperaccumulation in plants. Plants 8:. https://doi.org/10.3390/plants8010011

Villanueva López G, Martínez Surimendi P, Van der Wal H (2015) Árboles y arbustos en áreas ganaderas de Tabasco.pdf. Ecofronteras 54:14–17

Villaseñor JL (2016) Checklist of the native vascular plants of México. Rev Mex Biodivers 87:. https://doi.org/10.1016/j.rmb.2016.06.017

WCSP (2019) *World Checklist of Selected Plant Families*. Facilitated by the Royal Botanic Gardens, Kew. Published on the Internet; http://wcsp.science.kew.org/ Retrieved

CAPTIONS FOR FIGURES

Figure 1 Detail of *Blepharidium guatemalense* plants in the tropical forests of southeast Mexico. **a**. seeds*;* **b** fruit capsules*;* **c** inflorescences; **d** mature leaf of approximately 45 cm long and 18 cm wide; **e** detail of bark cutting showing a positive reaction to the field spot test based on DMG; **f** 25-m high individual.

Figure 2 Histogram indicating the frequency distribution of Ni concentration (µg g^{-1}) in herbarium specimens of *Blepharidium guatemalense* (*n*=182) analysed by X-ray fluorescence spectroscopy in MEXU, P and MO herbariums. The abscissa is plotted on a logarithmic scale.

Figure 3 Map showing the geographic distribution of *B. guatemalense* herbarium specimens analysed with XRF spectroscopy in the herbariums MEXU, P and MGB (number of voucher specimens with available geographic coordinates = 83). Ultramafic complexes are shown in black: Motozintla (Chiapas) and Polochic-Motahua (Guatemala). Geologic map sources: "Surface Geology of the Caribbean Region" of the USGC (United States Geological Survey) and Sistema Geológico Mexicano (SGM 2006, 2017).

Figure 4 Nickel concentrations in plant tissues of *B. guatemalense* presented as boxplots. Key symbols: open boxes are interquartile ranges, bold crosses are ± mean, whiskers are ± standard deviation and bold circles are outliers.

Figure 5 Biplot of the Principal Components Analysis (PCA) based on foliar elemental concentrations of *B. guatemalense* and the properties of its associated rhizosphere soils, n=21.

Figure 6 Elemental speciation of: **a** mature leaf (air-dried), **b** leaf detail and **c** seeds of *Blepharidium guatemalense*. Maps were generated using micro-XRF (20 µmx resolution). Mean concentrations in the leaf: 14 100 µg g^{-1} Ni, 3800 µg g^{-1} Ca, 17 900 µg g^{-1} K, 140 µg g^{-1} Fe and 190 µg g^{-1} Mn. Mean concentrations in seeds: 3280 µg g^{-1} Ca, 9680 µg g^{-1} K, 19 300 µg g^{-1} Ni.

Figure 7a X-ray fluorescence microscopy (XFM) elemental maps of leaf midrib cross-sections of *Blepharidium guatemalense*. Scan area is 3 x 1.8 mm (601 x 361 pixels) with a resolution of 5 microns and a per-pixel dwell of 9ms. Abbreviations of anatomical features: *xy*, xylem; *ph*, phloem; *c*, cortex; *sv*, secondary veins; *ue*, upper epidermis; *le*, lower epidermis; *mc*, midrib collenchyma.

Figure 7b X-ray fluorescence microscopy (XFM) elemental maps of a petiole cross-sections of *Blepharidium guatemalense*. Scan area is 2.5 x 2.3 mm (340 x 306 pixels) with a resolution of 3 microns and a per-pixel dwell of 4ms. Abbreviations of anatomical features: *xy*, xylem; *ph*, phloem; *co*, collenchyma; *sc*, sclerenchyma; *e*, epidermis.

Figure 7c X-ray fluorescence microscopy (XFM) elemental maps of a stem cross-sections of *Blepharidium guatemalense*. Scan area is 4.6 x 4.2 mm (782 x 692 pixels) with a resolution of 6 microns and a per-pixel dwell of 7ms. Abbreviations of anatomical features: *ox*, older xylem; *yx*, younger xylem; *op*, older phloem; *yp*, younger phloem; *c*, cortex; *e*, epidermis.

Figure 7d X-ray fluorescence microscopy (XFM) elemental maps of a root cross-section of *Blepharidium guatemalense*. Scan area is 2.7 x 2.5 mm (278 x 291 pixels) with a resolution of 5 microns and a per-pixel dwell of 5ms. Abbreviations of anatomical features: *xy*, xylem; *yx*, younger xylem; *ph*, phloem; *e*, epidermis; *en*, endodermis.

893

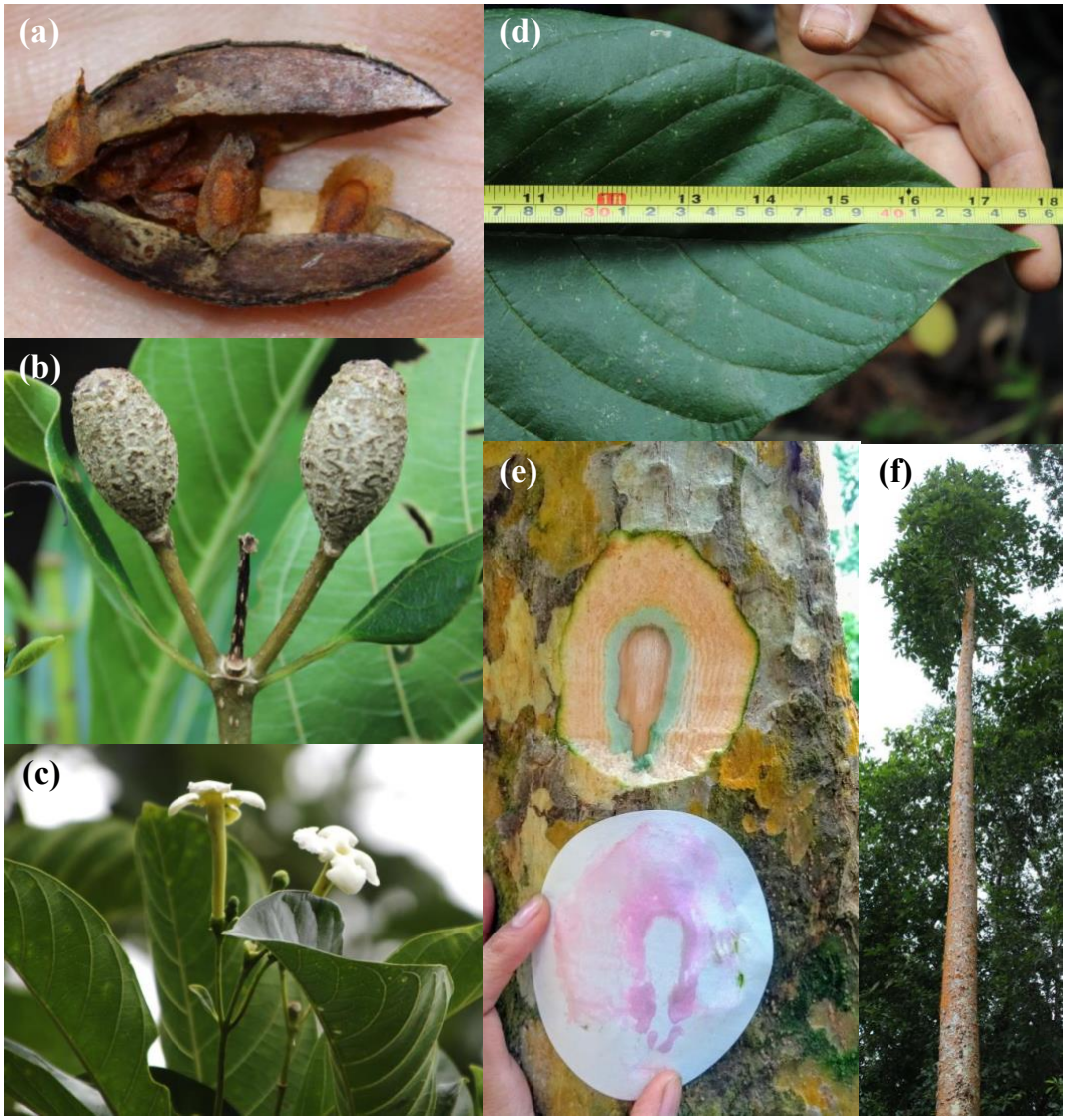

894
895 Figure 1

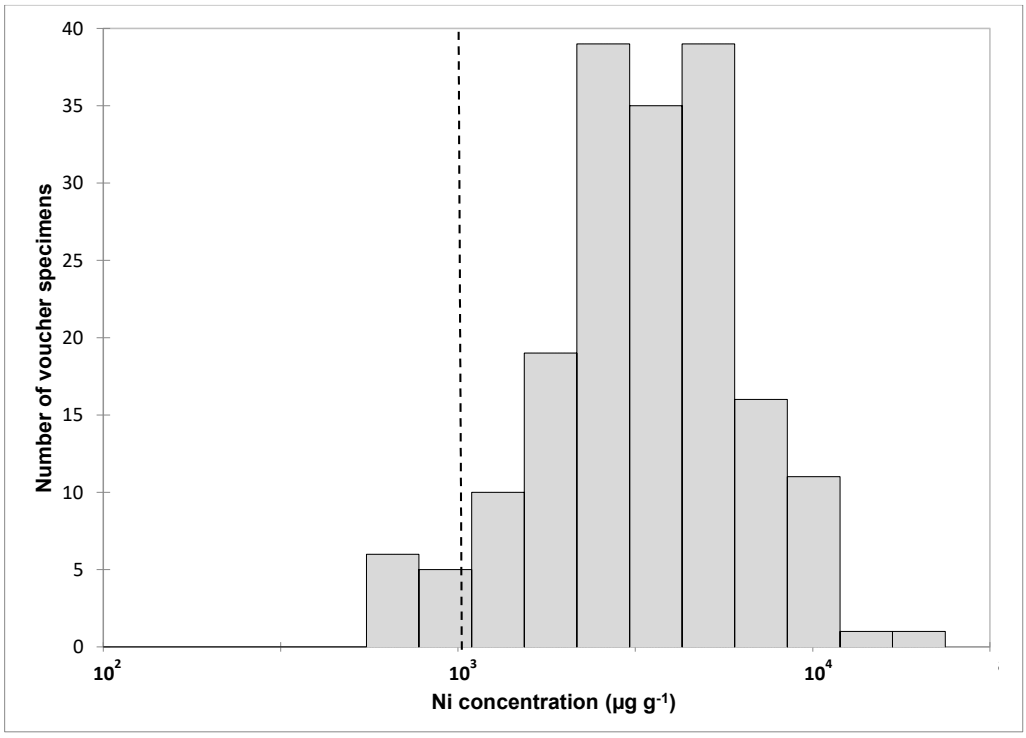

896
897 Figure 2

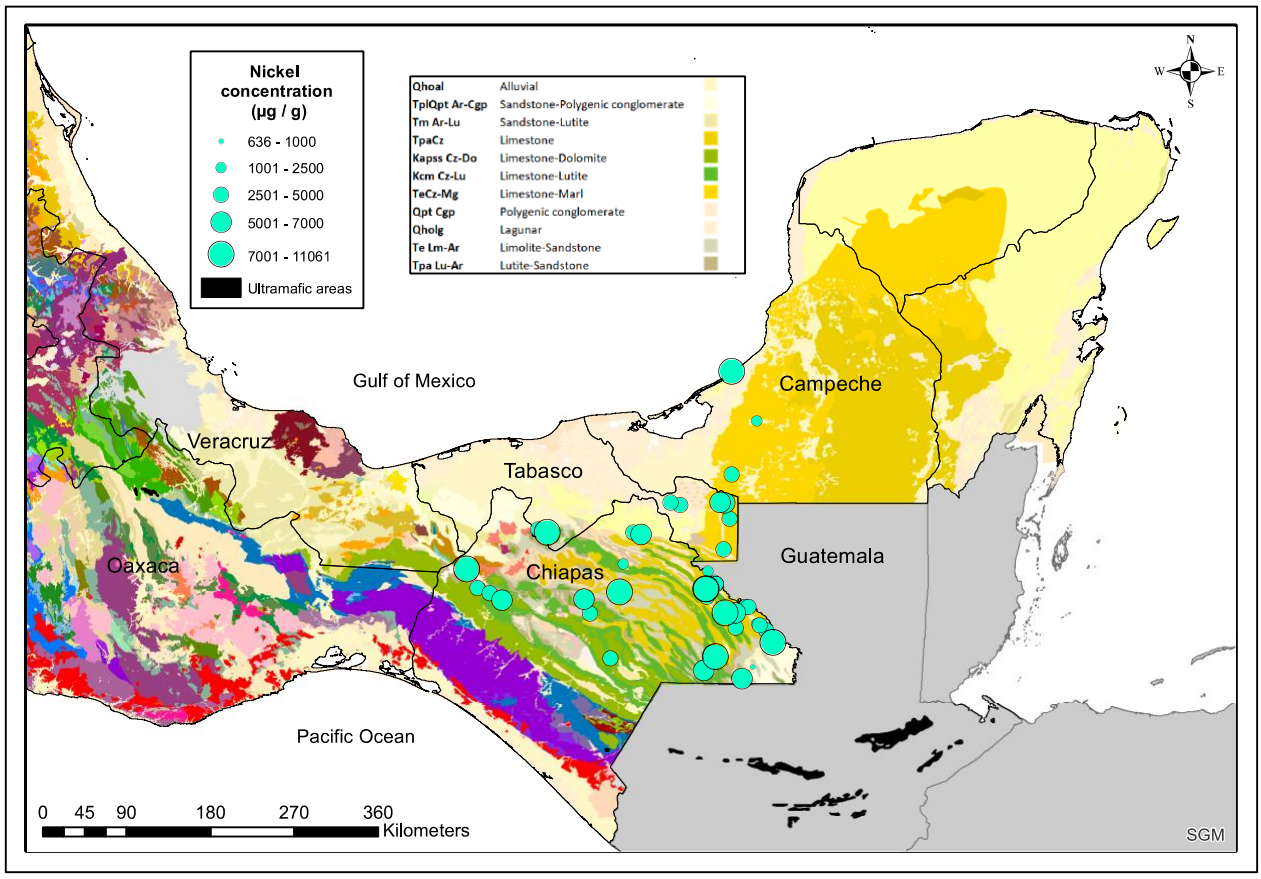

898
899 Figure 3

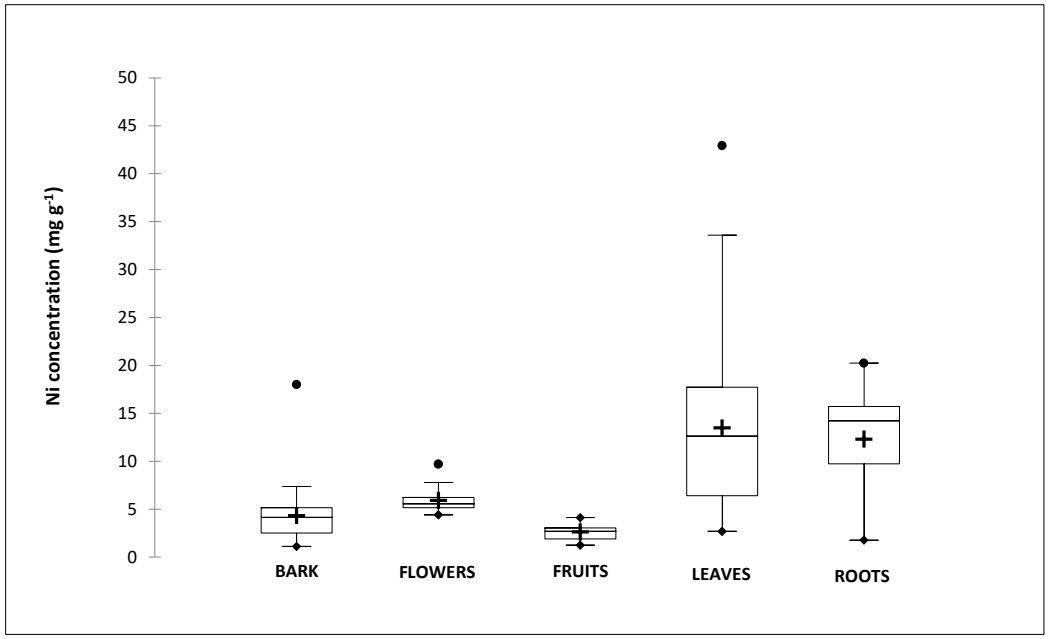

900
901 Figure 4

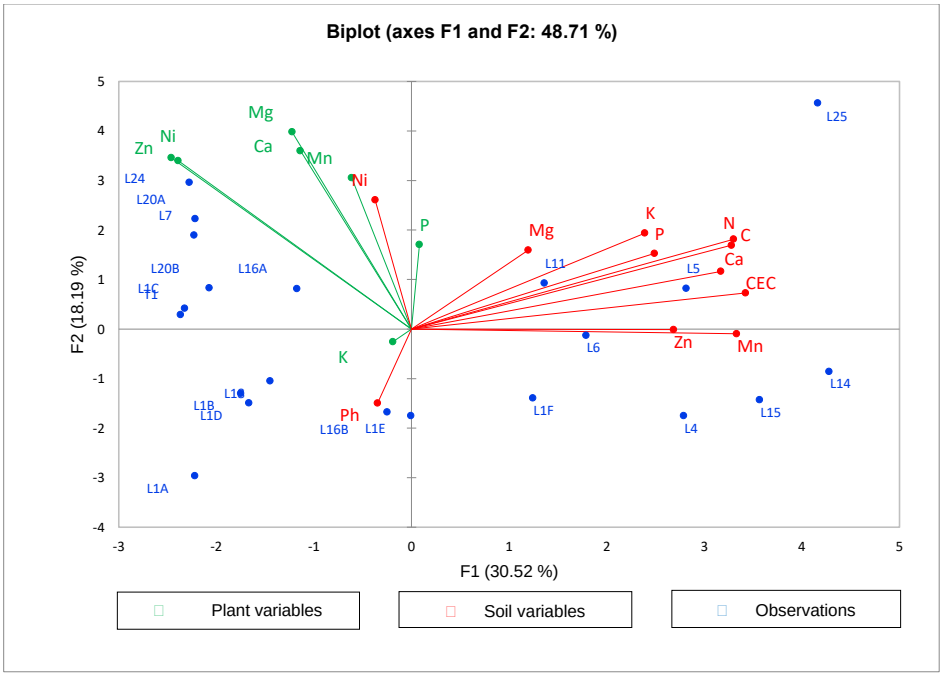

902
903 Figure 5

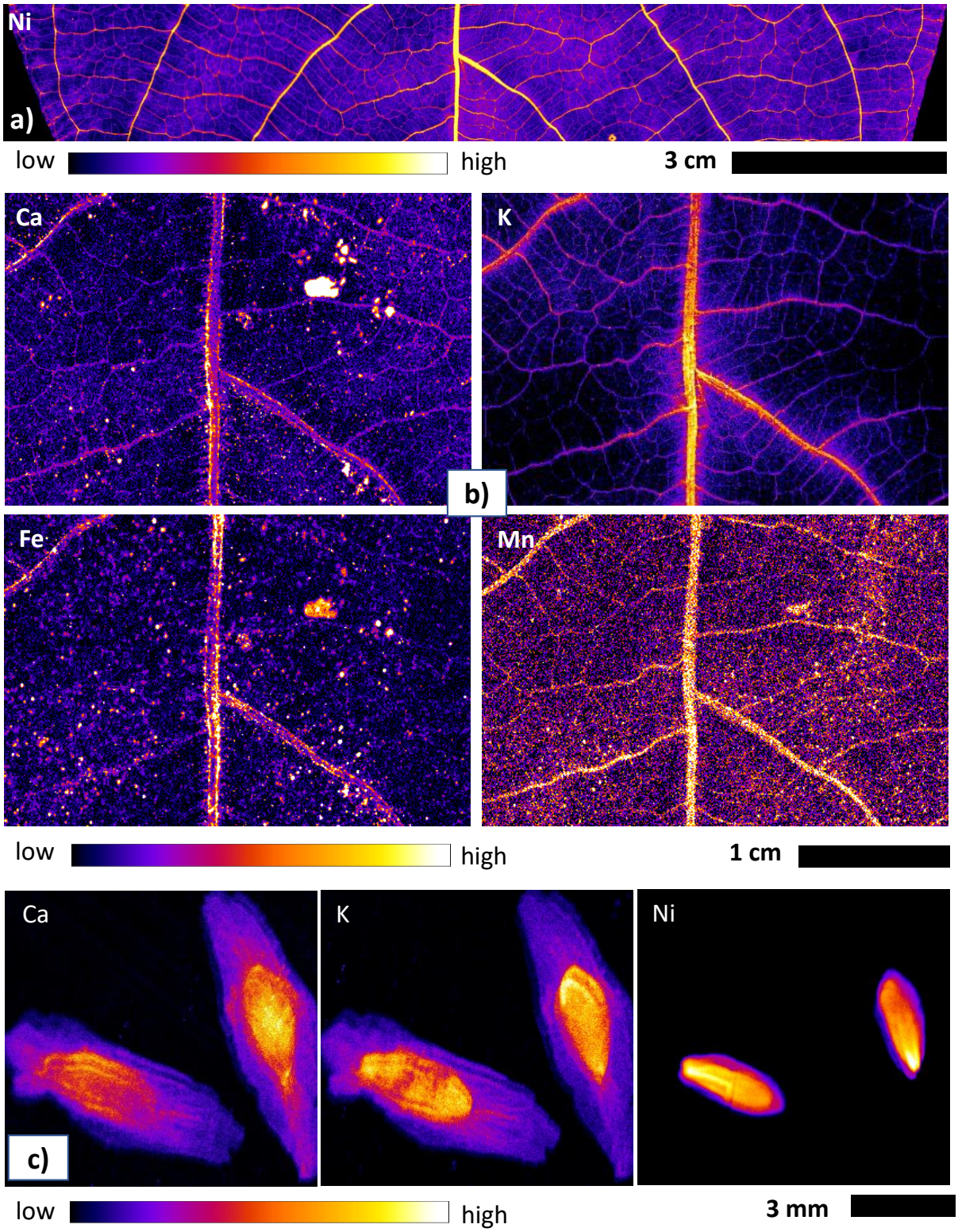

Figure 6

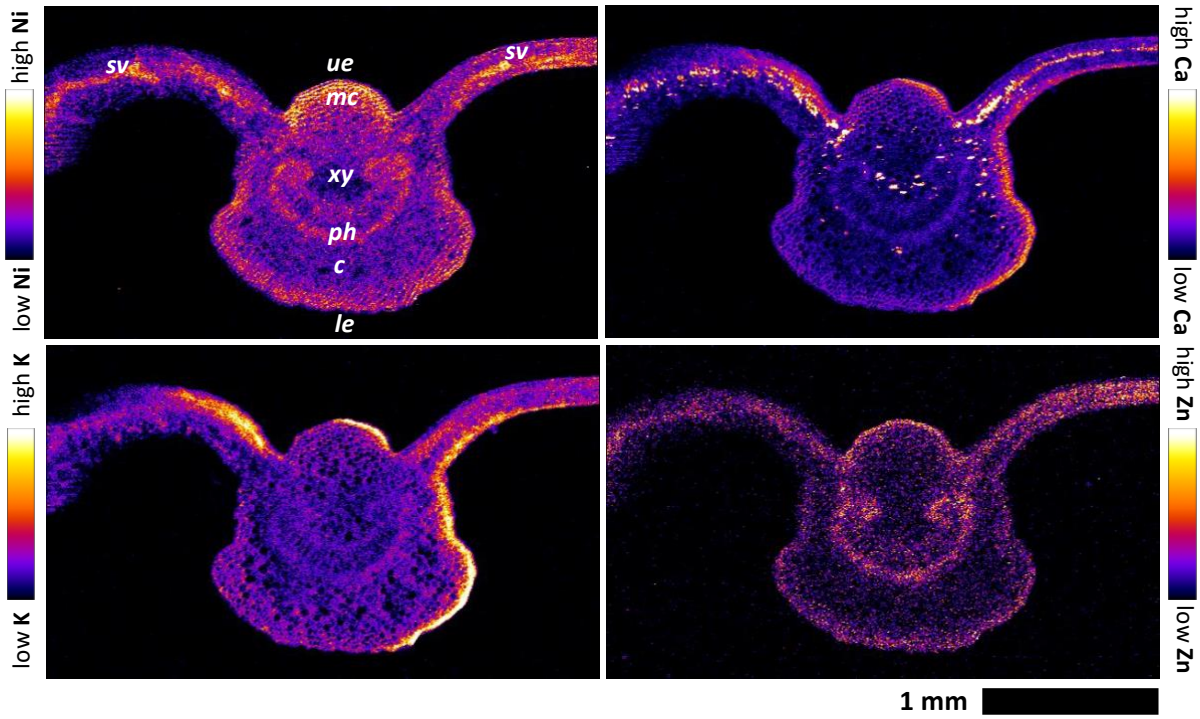
high Ni
low Ni
sv
ue
mc
sv
xy
ph
c
le
high Ca
low Ca
high K
low K
high Zn
low Zn
1 mm

Figure 7a

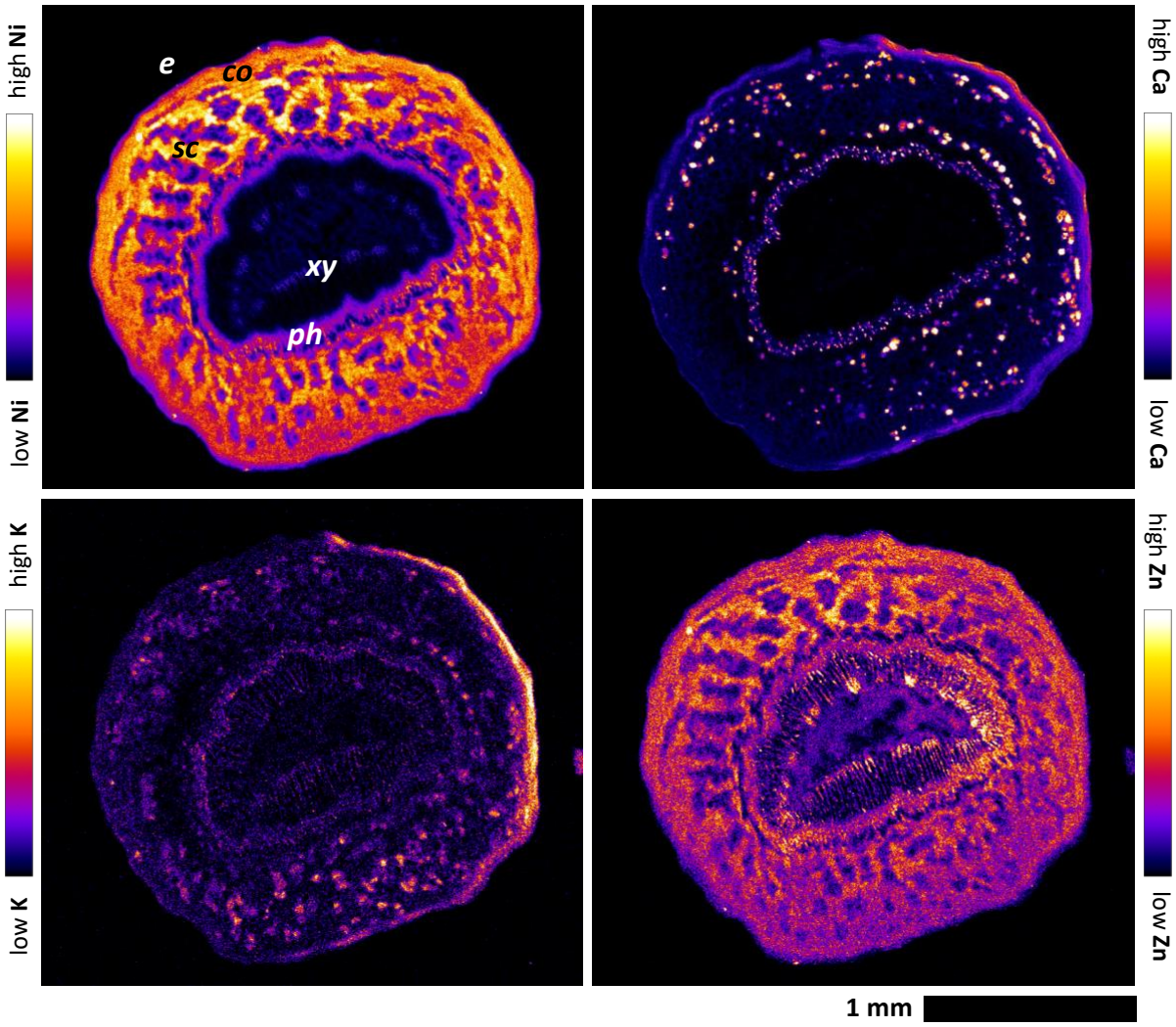

908
909 Figure 7b

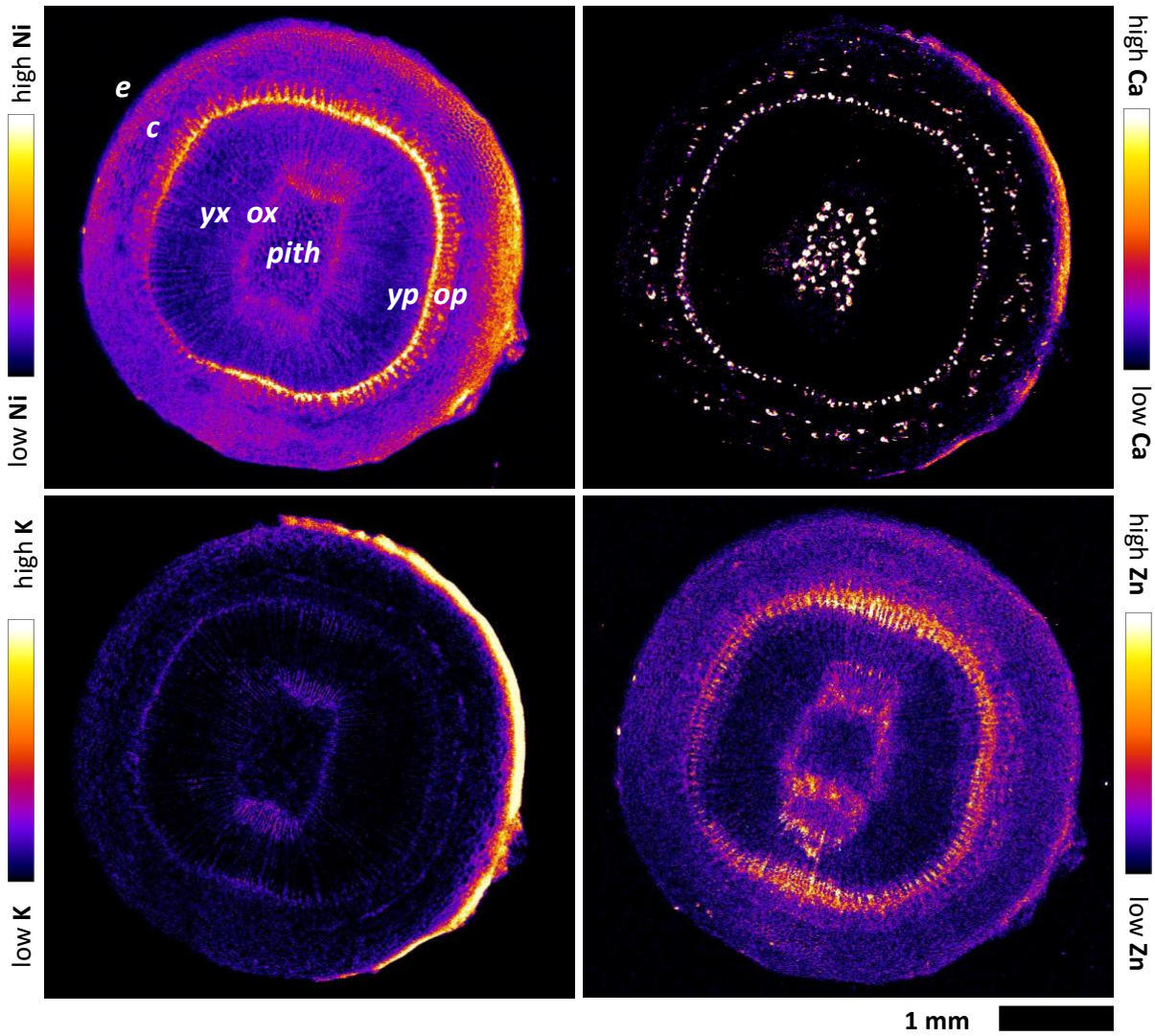

910
911 Figure 7c

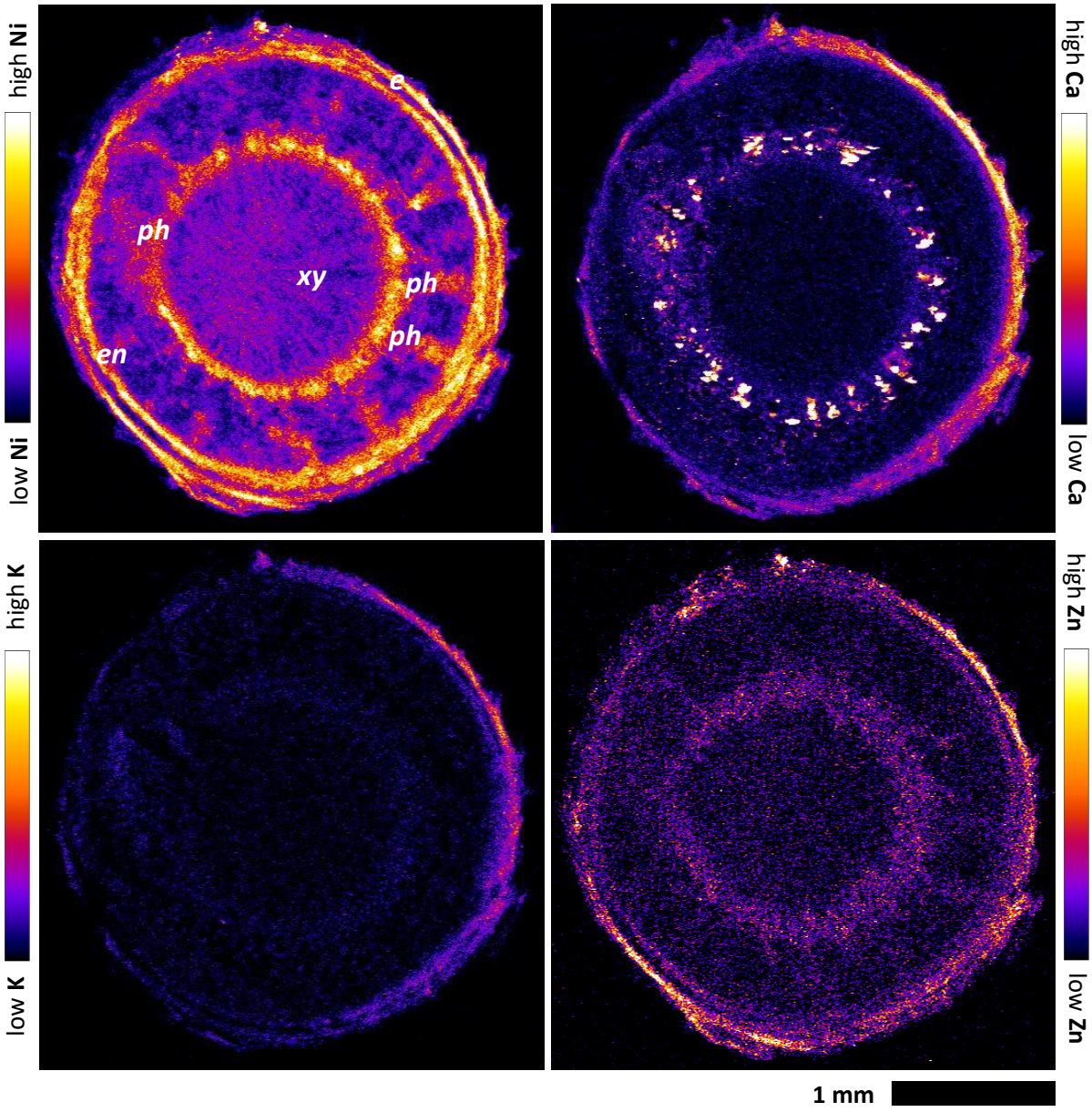

912
913 Figure 7d
914

915 **Table 1** Elemental concentrations in plant tissues of *B. guatemalense* from individuals collected in
916 their native habitat at Lacandonian rainforest (Chiapas, Mexico) and Tacotalpa (Tabasco, México).
917 The elemental concentrations are shown in ranges and means in μg g^{-1} (*n*= number of samples).
918

Plant part	***n***	**Elemental concentration (μg g^{-1})**					
		P	K	Ca	S	Al	Mg
Leaf	78	682–2150 (1210)	5700–28 900 (14 500)	2 990–14 200 (7200)	1730–7 060 (3070)	< 163–227 (85)	877–4700 (2260)
Flower	16	1790–2970 (2480)	13 500–24 200 (17 100)	2700–8850 (4835)	1680–2 660 (2370)	< 163	1650–5 490 (2440)
Seed	5	7730–10 300 (9050)	6420–10 600 (8630)	3110–3460 (3340)	2040-2340 (2210)	< 163	2610–3850 (3130)
Fruit	9	1490–2850 (2070)	13 400–26 400 (18 100)	1330–2690 (2090)	947–2050 (1340)	< 163–443 (122)	1190–2540 (1760)
Bark	25	178–1680 (606)	10700–54 600 (25 100)	3970–33 900 (16,800)	566–3910 (1660)	< 163–2960 (277)	274–2370 (743)
Root	11	232–532 (308)	5800–10 900 (7703)	4470–10 800 (7350)	719–4180 (2080)	1500–8380 (3910)	1170–2860 (1990)

919

Plant part	***n***	**Elemental concentration (μg g^{-1})**					
		Mn	Fe	Co	Cu	Ni	Zn
Leaf	78	22–587 (249)	< 50–561 (64)	7.4–149 (39)	< 0.6–22 (8.5)	2700–42 900 (13 500)	< 2.2–304 (96)
Flower	16	48–338 (112)	56–241 (83)	14–40 (24)	6.0–14 (11)	4420–9690 (5930)	44–80 (59)
Seed	5	217–297 (253)	< 50	27.4–44.2 (27.4)	< 0.6	16 700–19 800 (18 400)	< 2.2
Fruit	9	34–95 (61)	< 50–482 (133)	11–30 (17)	6.1–9.2 (7.8)	1260–4160 (2650)	17–56 (33)
Bark	25	36–764 (265)	< 50–333 (122)	1.9–116 (29)	< 0.6–10 (6.2)	1124–18 000 (4360)	20–215 (72)
Root	11	112–792 (447)	1460–6890 (4200)	11–120 (39)	6.9–23 (12)	1780–20 200 (12 300)	32–133 (99)

920
921

Table 2 Total and available elements of the rhizosphere soil collected in the native habitat of *B. guatemalense* at Lacandonian rainforest (Chiapas, Mexico). Concentrations are given in ranges and means in µg g^{-1} and the number of samples is 19.

Elements	Elemental concentrations (µg g^{-1})	
	Total	**DTPA-extractable**
Mg	5200–15 800 (10 500)	158–362 (247)
Ca	3550–14 900 (7360)	-
P	129–483 (287)	4.5–16 (9.4) *
K	1200–5560 (3370)	3.4–40 (18)
Al	20 900–67 700 (40 000)	< 0.8–9.6 (2.4)
Fe	36 500 –58 500 (45 300)	15–113 (54)
Mn	773–2660 (1380)	4.5–49 (25)
Cr	180–635 (310)	< 0.09
Co	28–101 (50)	< 0.08–1.8 (0.5)
Ni	240–1650 (610)	4.90–198 (50)
Zn	50–86 (65)	0.40–6.60 (2.9)

Soil pH is 5.91 – 7.36 (mean pH 6.53), *phosphorus using Olsen P extraction.

Appendix 1a Correlation matrix (Pearson) based on the foliar elemental concentrations of *B. guatemalense*. The values in bold are different from 0 at an alpha = 0.05 significance level (*n* = 21). For soil variables, we used DTPA-extractable elements for Mg, Mn, Ni and Zn.

	Ca	K	Mg	Mn	P	S	B	Co	Cu	Ni	Zn
Ca	1										
K	0.005	1									
Mg	0.807	0.053	1								
Mn	0.597	0.136	0.419	1							
P	-0.034	-0.066	0.066	0.370	1						
S	0.428	0.382	0.286	0.602	0.243	1					
B	0.178	-0.074	0.132	-0.194	-0.468	-0.134	1				
Co	0.245	0.574	0.150	0.331	-0.155	0.299	0.080	1			
Cu	0.186	0.022	0.317	0.036	0.262	0.165	0.018	0.120	1		
Ni	0.413	0.036	0.467	0.367	0.211	0.344	0.136	-0.097	0.326	1	
Zn	0.426	-0.098	0.508	0.334	0.268	0.227	0.169	-0.105	0.400	0.970	1

Appendix 1b Correlation matrix (Pearson) based on total elements contents from rhizosphere soils of *B. guatemalense*. The values in bold are different from 0 at an alpha = 0.05 significance level (*n* = 19).

Variables	*Al*	*Ca*	*Fe*	*K*	*Mg*	*Mn*	*P*	*S*	*As*	*B_*	*Cd*	*Co*	*Cr*	*Cu*	*Ni*	*Pb*	*Zn*
Al	**1**																
Ca	**0.540**	**1**															
Fe	**0.586**	0.160	**1**														
K	**0.616**	-0.029	0.246	**1**													
Mg	0.039	-0.205	-0.035	**0.504**	**1**												
Mn	-0.153	-0.413	0.169	0.214	0.155	**1**											
P	0.268	**0.602**	0.023	-0.105	-0.229	-0.389	**1**										
S	**0.589**	**0.918**	0.198	0.021	-0.372	-0.448	**0.704**	**1**									
As	**0.915**	**0.588**	**0.682**	**0.528**	0.053	-0.148	0.300	**0.572**	**1**								
*B_*	**0.486**	0.108	0.024	**0.837**	0.442	0.195	-0.311	0.106	0.365	**1**							
Cd	**0.802**	**0.505**	**0.521**	**0.569**	-0.003	-0.014	0.329	**0.491**	**0.873**	0.351	**1**						
Co	**-0.472**	**-0.605**	-0.148	-0.097	0.138	**0.775**	**-0.659**	**-0.657**	**-0.519**	0.060	**-0.475**	**1**					
Cr	**-0.620**	-0.347	0.044	**-0.647**	0.111	0.026	-0.096	**-0.470**	**-0.469**	**-0.752**	**-0.515**	0.230	**1**				
Cu	**0.798**	0.346	**0.541**	**0.711**	0.178	0.120	-0.020	0.348	**0.722**	**0.657**	**0.793**	-0.193	**-0.603**	**1**			
Ni	**-0.476**	-0.319	-0.231	-0.310	-0.053	0.041	-0.318	-0.376	-0.367	-0.253	-0.258	0.288	0.391	-0.299	**1**		
Pb	0.406	**0.458**	**0.591**	-0.202	**-0.605**	0.120	0.206	**0.534**	0.358	-0.143	0.285	-0.096	-0.106	0.308	-0.284	**1**	
Zn	0.352	-0.168	-0.031	**0.509**	0.188	0.109	-0.069	-0.061	0.209	0.404	0.148	0.117	-0.417	0.263	0.166	-0.263	**1**

Appendix 1c Correlation matrix (Pearson) based on the DTPA elemental contents and other variables from rhizosphere soils of *B. guatemalense*. The values in bold are different from 0 at an alpha = 0.05 significance level (*n* = 19).

Variables	*Al*	*Cd*	*Co*	*Cu*	*Fe*	*K*	*Mg*	*Mn*	*Na*	*Ni*	*Pb*	*Zn*	*CEC*	*P_s*	*N*	*C*	*Ph*
Al	**1**																
Cd	-0.114	**1**															
Co	0.070	0.426	**1**														
Cu	-0.040	**0.687**	0.325	**1**													
Fe	0.147	**0.652**	**0.789**	**0.695**	**1**												
K	0.049	**0.731**	0.291	**0.824**	**0.575**	**1**											
Mg	-0.167	0.193	-0.080	0.272	0.313	0.269	**1**										
Mn	-0.026	**0.710**	**0.761**	0.435	**0.712**	**0.603**	0.015	**1**									
Na	-0.127	0.254	0.015	0.399	0.389	0.125	0.450	0.011	**1**								
Ni	-0.210	0.112	0.278	0.396	0.229	0.249	-0.053	0.061	0.062	**1**							
Pb	-0.189	**0.722**	0.364	**0.740**	**0.753**	**0.580**	**0.542**	**0.498**	**0.718**	0.219	**1**						
Zn	-0.257	0.426	**0.689**	0.208	**0.605**	0.150	0.297	**0.537**	0.137	0.186	**0.501**	**1**					
CEC	-0.368	**0.725**	0.265	0.412	**0.554**	0.387	**0.463**	**0.485**	**0.519**	-0.068	**0.817**	**0.480**	**1**				
P_s	-0.022	**0.644**	**0.678**	**0.846**	**0.783**	**0.732**	0.052	**0.680**	0.208	**0.510**	**0.668**	0.400	0.362	**1**			
N	-0.234	**0.721**	0.343	0.377	**0.511**	0.387	0.274	**0.583**	**0.583**	0.094	**0.732**	**0.506**	**0.766**	0.371	**1**		
C	-0.256	**0.700**	0.271	0.363	**0.468**	0.435	0.379	**0.590**	**0.578**	0.031	**0.755**	**0.499**	**0.775**	0.349	**0.969**	**1**	
Ph	**-0.482**	0.011	**-0.500**	-0.283	**-0.553**	-0.241	-0.272	-0.166	-0.200	-0.287	-0.202	-0.312	0.164	-0.366	-0.007	0.025	**1**